

Stepwise Incorporation of Alkynes into a Coordinatively Unsaturated Diruthenium Center Bridged by Thiolate Ligands

Masayuki Nishio,[†] Hiroyuki Matsuzaka,[†] Yasushi Mizobe,[†] Tomoaki Tanase,[‡] and Masanobu Hidai^{*,†}

Department of Chemistry and Biotechnology, Faculty of Engineering, The University of Tokyo, Hongo, Tokyo 113, Japan, and Department of Chemistry, Faculty of Science, Toho University, Funabashi, Chiba 274, Japan

Received February 2, 1994[®]

The coordinatively unsaturated complex $\text{Cp}^*\text{Ru}(\mu_2\text{-SPr}^i)_2\text{RuCp}^*$ (**1**; $\text{Cp}^* = \eta^5\text{-C}_5\text{Me}_5$) readily reacts with an equimolar amount of $\text{HC}\equiv\text{CCO}_2\text{R}$ ($\text{R} = \text{Me}, \text{Et}, \text{Bu}^t$) at the diruthenium center to give dinuclear complexes with a ruthenathiacyclobutene core, $\text{Cp}^*\text{Ru}(\mu_2\text{-SPr}^i)[\eta^2:\eta^2-\mu_2\text{-C}(\text{CO}_2\text{R})=\text{CHSPr}^i]\text{RuCp}^*$ (**5a**, $\text{R} = \text{Me}$; **5b**, $\text{R} = \text{Et}$; **5c**, $\text{R} = \text{Bu}^t$). Subsequent treatment of **5a** with the series of alkynes $\text{HC}\equiv\text{CR}'$ ($\text{R}' = \text{CO}_2\text{Me}, \text{Tol}, \text{SiMe}_3; \text{Tol} = 4\text{-MeC}_6\text{H}_4$) results in the incorporation of another alkyne molecule into the diruthenium site in **5a**, affording either dinuclear ruthenacyclopentenyl complexes $\text{Cp}^*\text{Ru}(\mu_2\text{-SPr}^i)[\eta^2:\eta^3-\mu_2\text{-C}(\text{R}')\text{CHC}(\text{CO}_2\text{Me})=\text{CHSPr}^i]\text{RuCp}^*$ (**6a**, $\text{R}' = \text{CO}_2\text{Me}$; **6b**, $\text{R}' = \text{Tol}$) or the bridging alkyne complex $\text{Cp}^*\text{Ru}(\mu_2\text{-SPr}^i)(\mu_2\text{-H})[\eta^2:\eta^2-\mu_2\text{-R'C=CC}(\text{CO}_2\text{Me})=\text{CHSPr}^i]\text{RuCp}^*$ (**7**; $\text{R}' = \text{SiMe}_3$). From **6**, two types of dinuclear ruthenacyclopentadiene complexes are obtained by the reactions with MeI: the neutral diiodo complex $\text{Cp}^*\text{I}_2\text{Ru}[\eta^2:\eta^4-\mu_2\text{-C}(\text{CO}_2\text{Me})\text{CHC}(\text{CO}_2\text{Me})\text{CH}]\text{RuCp}^*$ (**8**) from **6a** and the cationic complex $[\text{Cp}^*\text{Ru}(\mu_2\text{-SPr}^i)\{\eta^2:\eta^4-\mu_2\text{-C}(\text{Tol})\text{CHC}(\text{CO}_2\text{Me})\text{CH}\}]\text{RuCp}^*\text{I}$ (**10a**) from **6b**. A dimethyl analogue of **8**, $\text{Cp}^*\text{Me}_2\text{Ru}[\eta^2:\eta^4-\mu_2\text{-C}(\text{CO}_2\text{Me})\text{CHC}(\text{CO}_2\text{Me})\text{CH}]\text{RuCp}^*$ (**9**), is further derived from **8** upon treatment with LiCuMe_2 . On the other hand, oxidation of the alkyne complex **7** with I_2 results in the release of the coordinated alkyne $\text{Me}_3\text{SiC}\equiv\text{CC}(\text{CO}_2\text{Me})=\text{CHSPr}^i$ (**11**). Structures of **5c**, **6a**, **7**, **9**, and **10b** (PF_6^- salt of the cation in **10a**) have been unambiguously established by X-ray diffraction studies. Crystal data: **5c**, triclinic, $P\bar{1}$, $a = 11.2375(9)$ Å, $b = 17.876(4)$ Å, $c = 9.079(2)$ Å, $\alpha = 94.70(3)^\circ$, $\beta = 105.54(1)^\circ$, $\gamma = 92.01(1)^\circ$, $Z = 2$, 5596 reflections, $R = 0.051$, $R_w = 0.058$; **6a**, triclinic, $P\bar{1}$, $a = 10.999(3)$ Å, $b = 19.155(4)$ Å, $c = 9.139(2)$ Å, $\alpha = 102.22(1)^\circ$, $\beta = 107.96(2)^\circ$, $\gamma = 78.28(2)^\circ$, $Z = 2$, 5448 reflections, $R = 0.045$, $R_w = 0.057$; **7**, triclinic, $P\bar{1}$, $a = 11.323(3)$ Å, $b = 17.356(3)$ Å, $c = 10.627(2)$ Å, $\alpha = 101.80(1)^\circ$, $\beta = 109.79(2)^\circ$, $\gamma = 80.78(2)^\circ$, $Z = 2$, 2352 reflections, $R = 0.079$, $R_w = 0.051$; **9**, orthorhombic, $P2_12_12_1$, $a = 16.412(5)$ Å, $b = 16.650(6)$ Å, $c = 10.594(3)$ Å, $Z = 4$, 1956 reflections, $R = 0.049$, $R_w = 0.036$; **10b**· $\text{ClCH}_2\text{CH}_2\text{Cl}$, triclinic, $P\bar{1}$, $a = 12.537(2)$ Å, $b = 18.442(2)$ Å, $c = 9.2737(9)$ Å, $\alpha = 95.105(9)^\circ$, $\beta = 96.545(9)^\circ$, $\gamma = 94.81(1)^\circ$, $Z = 2$, 5103 reflections, $R = 0.068$, $R_w = 0.088$.

Introduction

Multicentered activation of organic substrates by polynuclear transition-metal complexes is an attractive approach to the new types of chemical transformations which are inaccessible on mononuclear metal centers.¹ In this context, transition-metal–sulfur cluster compounds can serve as suitable templates, since the strong bridging behavior of sulfur ligands can inhibit the fragmentation of the polynuclear structure even under forcing reaction conditions. However, although transition-metal–sulfur compounds have been studied intensively because of their relevance to biological and industrial catalytic processes, including electron transfer and desulfurization,² organic syntheses at the poly-

metallic site in metal–sulfur aggregates have still been poorly investigated.³

We have recently established general synthetic routes to a series of dinuclear Cp^*Ru complexes ($\text{Cp}^* = \eta^5\text{-C}_5\text{Me}_5$) with bridging thiolate ligands.^{4–6} Our current interest has been focused on developing novel modes of activation and transformation of organic substrates on these well-defined thiolate-bridged diruthenium centers. Among the diruthenium complexes isolated to date, $\text{Cp}^*\text{Ru}(\mu_2\text{-SPr}^i)_2\text{RuCp}^*$ (**1**)^{4c,7} appears to be the most

(2) (a) *Adv. Inorg. Chem.* **1992**, *38*. (b) Berg, J. M.; Holm, R. H. In *Metal Ions in Biology*; Spiro, T. G., Ed.; Wiley: New York, 1982; Vol. 4, pp 1–66. (c) Rauchfuss, T. B. *Prog. Inorg. Chem.* **1991**, *39*, 259. (d) Angelici, R. J. *J. Acc. Chem. Res.* **1988**, *21*, 387. (e) Rakowski DuBois, M. *Chem. Rev.* **1989**, *89*, 1.

(3) For pertinent examples, see: (a) Seydel, D.; Anderson, L. L.; Villafañe, F.; Cowie, M.; Hilts, R. W. *Organometallics* **1992**, *11*, 3262. (b) Claver, C.; Fis, J.; Kalck, P.; Jaud, J. *Inorg. Chem.* **1987**, *26*, 3479. (c) El Amane, M.; Maisonnat, A.; Dahan, F.; Pince, R.; Poilblanc, R. *Organometallics* **1985**, *4*, 773. (d) Adams, R. D.; Babin, J. E.; Tasi, M.; Wang, J.-G. *Organometallics* **1988**, *7*, 755.

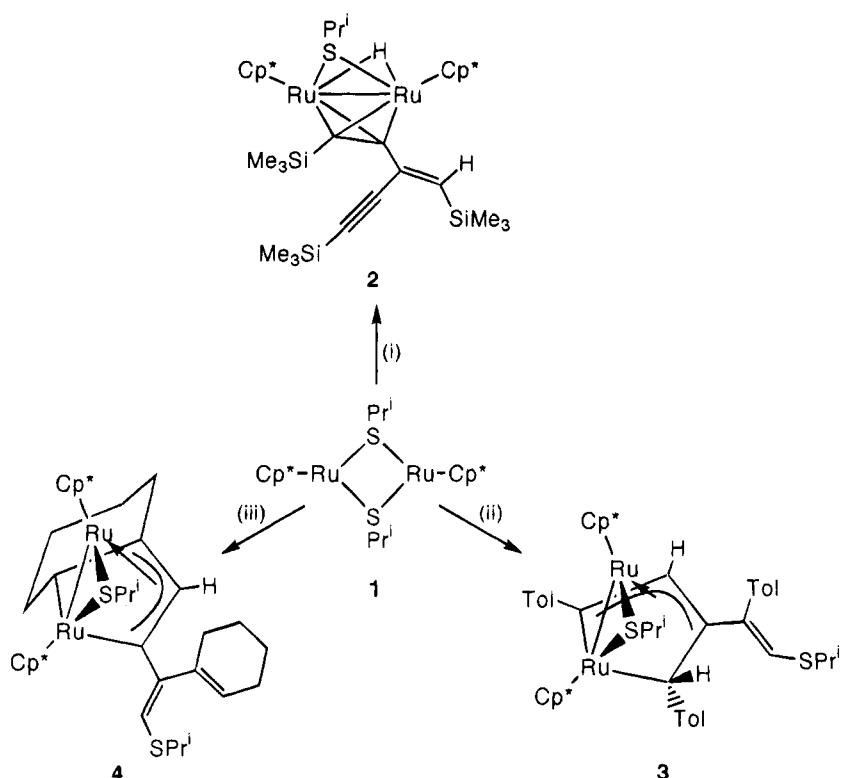
(4) (a) Dev, S.; Imagawa, K.; Mizobe, Y.; Cheng, G.; Wakatsuki, Y.; Yamazaki, H.; Hidai, M. *Organometallics* **1989**, *8*, 1232. (b) Dev, S.; Mizobe, Y.; Hidai, M. *Inorg. Chem.* **1990**, *29*, 4797. (c) Takahashi, A.; Mizobe, Y.; Matsuzaka, H.; Dev, S.; Hidai, M. *J. Organomet. Chem.* **1993**, *456*, 243. (d) Hidai, M.; Mizobe, Y.; Matsuzaka, H. *J. Organomet. Chem.* **1994**, *473*, 1.

[†] The University of Tokyo.

[‡] Toho University.

^{*} Abstract published in *Advance ACS Abstracts*, September 1, 1994.

(1) Recent reviews: (a) *The Chemistry of Metal Cluster Complexes*; Shriver, D. F., Kaesz, H. D., Adams, R. D., Eds.; VCH: Weinheim, Germany, 1990. (b) Braunstein, P.; Rose, J. In *Chemical Bonds—Better Ways to Make Them and Break Them*; Bernal, I., Ed.; Elsevier: Amsterdam, 1989. (c) Adams, R. D.; Horvath, I. T. *Prog. Inorg. Chem.* **1985**, *33*, 127.

Scheme 1^a

^a Reagents: (i) $\text{HC}\equiv\text{CSiMe}_3$; (ii) $\text{HC}\equiv\text{CTol}$; (iii) $\text{HC}\equiv\text{CC}=\text{CH}(\text{CH}_2)_3\text{CH}_2$.

promising template, since the adjacent 16-electron Ru (II) centers in **1** are expected to provide the unique bimetallic reaction site. Indeed, **1** has proved to incorporate readily a variety of substrates such as alkynes, CO, Bu^4NC , H_2 , and organic halides into the dinuclear site.^{4c,8,9} Particularly interesting is its unique reactivity with terminal alkynes, which is surprisingly sensitive to the alkyne substituent. As shown in Scheme 1, the reaction of **1** with $\text{HC}\equiv\text{CSiMe}_3$ leads to unusual oxidative trimerization of the alkyne to afford the bridging alkyne complex $\text{Cp}^*\text{Ru}(\mu_2\text{-SPr}^i)(\mu_2\text{-H})[\eta^2\text{-}\eta^2\text{-}\mu_2\text{-Me}_3\text{-SiMe}_3]$

(5) Recent examples of ruthenium–sulfur compounds: (a) Houser, E. J.; Amarasekera, J.; Rauchfuss, T. B.; Wilson, S. R. *J. Am. Chem. Soc.* **1991**, *113*, 7440. (b) Rauchfuss, T. B.; Rodgers, D. P. S.; Wilson, S. R. *J. Am. Chem. Soc.* **1986**, *108*, 3114. (c) Shaver, A.; Plouffe, P. Y.; Liles, D. C.; Singleton, E. *Inorg. Chem.* **1992**, *31*, 997. (d) Kawano, M.; Uemura, H.; Watanabe, T.; Matsumoto, K. *J. Am. Chem. Soc.* **1993**, *115*, 2068. (e) Schacht, H. T.; Haltiwanger, R. C.; Rakowski DuBois, M. *Inorg. Chem.* **1992**, *31*, 1728. (f) Mashima, K.; Mikami, A.; Nakamura, A. *Chem. Lett.* **1992**, 1473. (g) Brunner, H.; Janietz, N.; Wachter, J.; Nuber, B.; Ziegler, M. L. *J. Organomet. Chem.* **1988**, *356*, 85. (h) Koch, S. A.; Millar, M. *J. Am. Chem. Soc.* **1983**, *105*, 3362.

(6) Some dinuclear ruthenium complex with Cp or Cp^* ligands have recently been reported: (a) Kuhlman, R.; Streib, K.; Caulton, K. G. *J. Am. Chem. Soc.* **1993**, *115*, 5813. (b) Lin, W.; Wilson, S. R.; Girolami, G. S. *J. Chem. Soc., Chem. Commun.* **1993**, 284. (c) Suzuki, H.; Takao, T.; Tanaka, M.; Moro-Oka, Y. *J. Chem. Soc., Chem. Commun.* **1992**, 476. (d) Kölle, U.; Kang, B.-S.; Thewalt, U. *Organometallics* **1992**, *11*, 2893. (e) Hubbard, J. L.; Morneau, A.; Burns, R. M.; Zolch, C. R. *J. Am. Chem. Soc.* **1991**, *113*, 9176. (f) Knox, S. A. R. *J. Organomet. Chem.* **1990**, *400*, 255 and references cited therein. (g) Loren, S. D.; Campion, B. K.; Heyn, R. H.; Tilley, T. D.; Bursten, B. E.; Luth, K. W. *J. Am. Chem. Soc.* **1989**, *111*, 4712. (h) Chang, J. C.; Bergman, R. G. *J. Am. Chem. Soc.* **1987**, *109*, 4298.

(7) Recently Kölle and co-workers independently reported the synthesis and crystal structure of $\text{Cp}^*\text{Ru}(\mu_2\text{-SEt}_2)\text{RuCp}^*$ ($\text{Cp}^* = \eta^5\text{-C}_5\text{Me}_5\text{Et}$): Kölle, U.; Rietmann, C.; Englert, U. *J. Organomet. Chem.* **1992**, *423*, C20.

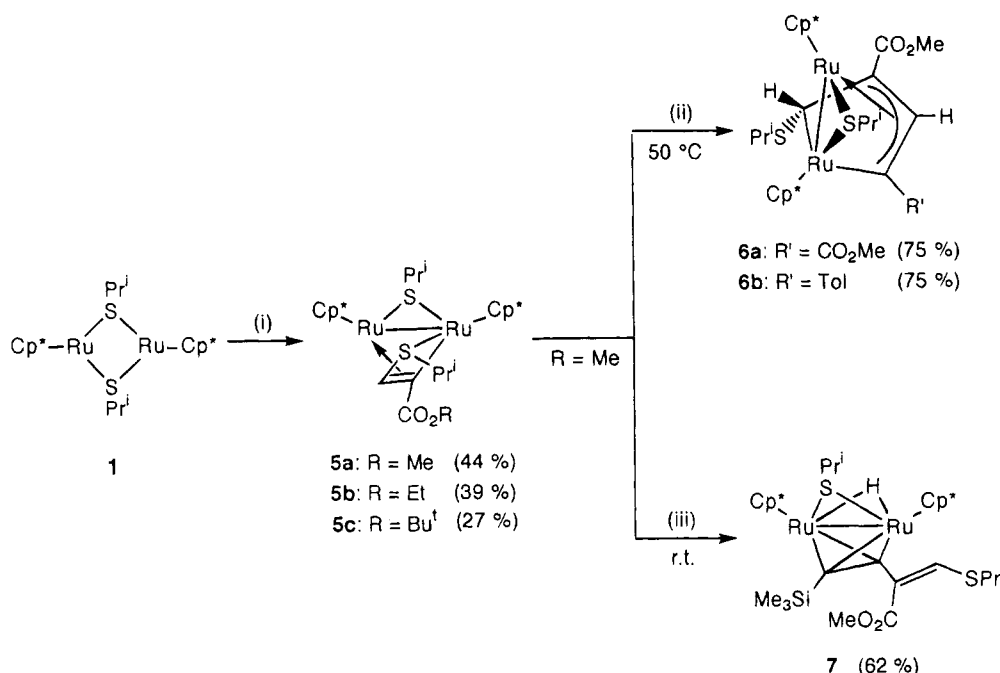
(8) (a) Matsuzaka, H.; Mizobe, Y.; Nishio, M.; Hidai, M. *J. Chem. Soc., Chem. Commun.* **1991**, 1101. (b) Nishio, M.; Matsuzaka, H.; Mizobe, Y.; Hidai, M. *J. Chem. Soc., Chem. Commun.* **1993**, 375.

(9) Hoernig, A.; Rietmann, C.; Englert, U.; Wagner, T.; Kölle, U. *Chem. Ber.* **1993**, *126*, 2609.

$\text{SiC}=\text{CC}(\text{C}=\text{CSiMe}_3=\text{CHSiMe}_3)\text{RuCp}^*$ (**2**),^{8a} whereas reactions with $\text{HC}\equiv\text{CR}$ ($\text{R} = \text{Tol}$, $\text{C}=\text{CH}(\text{CH}_2)_3\text{CH}_2$) result in the formal insertion of *three* (for $\text{R} = \text{Tol}$) or *two* (for $\text{R} = \text{C}=\text{CH}(\text{CH}_2)_3\text{CH}_2$) alkyne molecules into the $\text{Ru}-\text{S}$ bond in **1** accompanied by ring closure, forming the dinuclear ruthenacyclopentenyl complexes $\text{Cp}^*\text{Ru}(\mu_2\text{-SPr}^i)[\eta^2\text{-}\eta^3\text{-}\mu_2\text{-CH(R)C}\{\text{C}(\text{R})=\text{CHSPr}^i\}\text{CHC(R)}]\text{RuCp}^*$ (**3**; $\text{R} = \text{Tol}$) and $\text{Cp}^*\text{Ru}(\mu_2\text{-SPr}^i)[\eta^2\text{-}\eta^3\text{-}\mu_2\text{-C}\{\text{C}(\text{R})=\text{CHSPr}^i\}\text{CHC}\{(\text{CH}_2)_3\text{CH}_2\}\text{CH}]\text{RuCp}^*$ (**4**; $\text{R} = \text{C}=\text{CH}(\text{CH}_2)_3\text{CH}_28b,10 respectively. However, we could not elucidate the mechanisms of these reactions, since no intermediates were isolated or detected even from the reactions of **1** with a limited amount of these alkynes at low temperatures.$

Now we have found that the extension of the alkyne to $\text{HC}\equiv\text{CCO}_2\text{Me}$ in the reaction with **1** results in the isolation of a new type of dinuclear ruthenacyclopentenyl complex, $\text{Cp}^*\text{Ru}(\mu_2\text{-SPr}^i)[\eta^2\text{-}\eta^3\text{-}\mu_2\text{-C}(\text{CO}_2\text{Me})\text{CHC}(\text{CO}_2\text{Me})\text{CHSPr}^i]\text{RuCp}^*$ (**6a**). Furthermore, the reaction of **1** with an equimolar amount of this alkyne afforded the dinuclear complex $\text{Cp}^*\text{Ru}(\mu_2\text{-SPr}^i)[\eta^2\text{-}\eta^2\text{-}\mu_2\text{-C}(\text{CO}_2\text{Me})=\text{CHSPr}^i]\text{RuCp}^*$ (**5a**), which has been confirmed to be the intermediate for the formation of **6a** from **1**. We wish to report herein the details of **5** and a series of diruthenium complexes derived from **5a**, including

(10) Transformations of alkynes with a series of dinuclear Cp^*Ru -thiolate complexes have been investigated in detail in this laboratory. Interestingly, these reactions are surprisingly sensitive to the nature of the diruthenium site and the alkyne substituents. See: (a) Matsuzaka, H.; Hirayama, Y.; Nishio, M.; Mizobe, Y.; Hidai, M. *Organometallics* **1993**, *12*, 36. (b) Matsuzaka, H.; Koizumi, H.; Takagi, Y.; Nishio, M.; Hidai, M. *J. Am. Chem. Soc.* **1993**, *115*, 10396. (c) Matsuzaka, H.; Takagi, Y.; Hidai, M. *Organometallics* **1994**, *13*, 13.

Scheme 2^a

^a Reagents: (i) $\text{HC}\equiv\text{CCO}_2\text{R}$; (ii) $\text{HC}\equiv\text{CR}'$; (iii) $\text{HC}\equiv\text{CSiMe}_3$.

dinuclear ruthenacyclopentenyl, ruthenacyclopentadiene, and bridging alkyne complexes **6**, **8**, **10**, and **7**.

Results and Discussion

Reactions of $\text{Cp}^*\text{Ru}(\mu_2\text{-SPri})_2\text{RuCp}^*$ (1) with $\text{HC}\equiv\text{CCO}_2\text{R}$ (R = Me, Et, Bu^t) To Form Dinuclear Complexes 5 with a Ruthenathiacyclobutene Core. A dark blue toluene solution of **1** immediately turned to dark brown upon addition of $\text{HC}\equiv\text{CCO}_2\text{R}$ (1 equiv) at room temperature. Subsequent workup resulted in the isolation of dinuclear complexes possessing a four-membered RuC₂S ring, $\text{Cp}^*\text{Ru}(\mu_2\text{-SPri})[\eta^2\text{-}\mu^2\text{-C}(\text{CO}_2\text{R})=\text{CHSPri}]\text{RuCp}^*$ (**5a**, R = Me; **5b**, R = Et; **5c**, R = Bu^t) (Scheme 2) as green crystalline solids. The structure of **5c** has been characterized by X-ray crystallography (Figure 1). The ¹H NMR spectrum of **5c** is consistent with this structure, showing characteristic Cp* (δ 1.95, 1.79) and olefinic (δ 4.60) proton resonances together with those due to Bu^t and two inequivalent SPri groups. The ¹³C{¹H} NMR spectrum of **5c** exhibits a resonance at δ 126.32 attributable to the olefinic carbon having a CO_2Bu^t substituent, as well as the other

(11) (a) Seyferth, D.; Hoke, J. B.; Womack, G. B. *Organometallics* **1990**, *9*, 2662. (b) Seyferth, D.; Hoke, J. B.; Wheeler, D. R. *J. Organomet. Chem.* **1988**, *341*, 421. (c) Seyferth, D.; Hoke, J. B.; Dewan, J. C. *Organometallics* **1987**, *6*, 895.

(12) Davidson, J. L.; Harrison, W.; Sharp, D. W. A.; Sim, G. A. *J. Organomet. Chem.* **1972**, *46*, C47.

(13) Devillers, J.; Bonnet, J.-J.; de Montauzon, D.; Galy, J.; Poilblanc, R. *Inorg. Chem.* **1980**, *19*, 154.

(14) (a) Agh-Atabay, N. M.; Davidson, J. L. *J. Chem. Soc., Dalton Trans.* **1992**, 3531. (b) Carlton, L.; Agh-Atabay, N. M.; Davidson, J. L. *J. Organomet. Chem.* **1991**, *413*, 205. (c) Carlton, L.; Bakar, W. A. W. A.; Davidson, J. L. *J. Organomet. Chem.* **1990**, *394*, 177. (d) Bakar, W. A. W. A.; Carlton, L.; Davidson, J. L.; Manojlović-Muir, Lj.; Muir, K. W. *J. Organomet. Chem.* **1988**, *352*, C54. (e) Petillon, F. Y.; Le Froch-Perennou, F.; Guerchais, J. E.; Sharp, D. W. A. *J. Organomet. Chem.* **1979**, *173*, 89. (f) Guerchais, J. E.; Le Froch-Perennou, F.; Petillon, F. Y.; Keith, a. N.; Manojlović-Muir, Lj.; Muir, K. W.; Sharp, D. W. A. *J. Chem. Soc., Chem. Commun.* **1979**, *410*. (g) Davidson, J. L.; Sharp, D. W. A. *J. Chem. Soc., Dalton Trans.* **1975**, 2283.

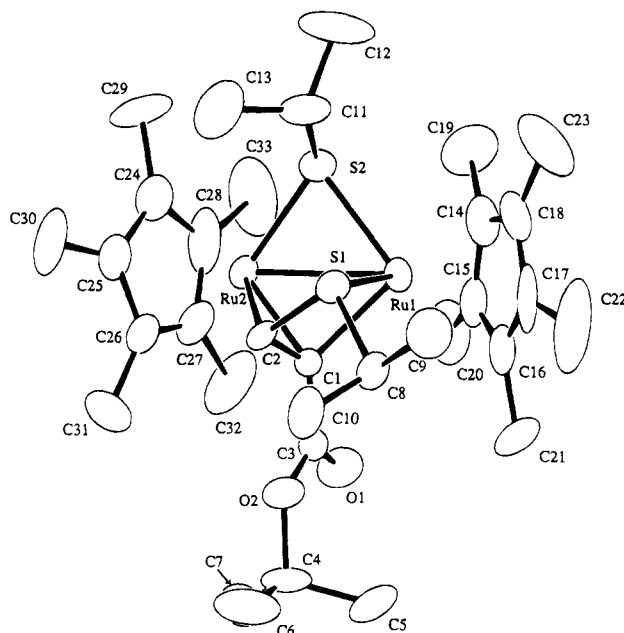


Figure 1. Molecular structure of **5c**, showing the atom-labeling scheme. The thermal ellipsoids are drawn at the 50% probability level.

olefinic, Cp*, SPri, and CO_2Bu^t resonances. The NMR spectral features of **5a** and **5b** are essentially similar to those of **5c** (see Experimental Section).

Although interactions of alkynes with transition-metal–thiolate complexes have been reported by several groups,^{11–14} this is, to our knowledge, the first example of the formation of dinuclear complexes having a metallathiacyclobutene framework.¹⁵ Analogous insertion of $\text{CF}_3\text{C}\equiv\text{CCF}_3$ into the M–S bond was previously observed for the dimanganese complex $(\text{OC})_4\text{Mn}(\mu_2\text{-SC}_6\text{-})$

(15) Complexes containing a bridging four-membered metallathiacyclic structure such as **5** are still rare. Diiron complexes having the related MC_2S ring are known, which have been prepared by routes quite different from that for **5**.¹⁶

Table 1. X-ray Crystallographic Data for 5c, 6a, 7, 9, and 10b-ClCH₂CH₂Cl

	5c	6a	7	9	10b-ClCH ₂ CH ₂ Cl
(A) Crystal Data					
formula	C ₃₃ H ₅₄ O ₂ S ₂ Ru ₂	C ₃₄ H ₅₂ O ₂ S ₂ Ru ₂	C ₃₅ H ₅₈ O ₂ SiS ₂ Ru ₂	C ₃₀ H ₄₄ O ₄ Ru ₂	C ₃₈ H ₅₃ O ₂ SRu ₂ PF ₆ Cl ₂
mol wt	749.05	791.05	805.19	670.82	991.91
space group	P <bar>1</bar>	P <bar>1</bar>	P <bar>1</bar>	P ₂ 12 ₁ 2 ₁	P <bar>1</bar>
cryst syst	triclinic	triclinic	triclinic	orthorhombic	triclinic
crystal color	green	yellow-green	dark red	orange	dark red
a, Å	11.2375(9)	10.999(3)	11.323(3)	16.412(5)	12.537(2)
b, Å	17.876(4)	19.155(4)	17.356(3)	16.650(6)	18.442(2)
c, Å	9.079(2)	9.139(2)	10.627(2)	10.594(3)	9.2737(9)
α, deg	94.70(3)	102.22(1)	101.80(1)		95.105(9)
β, deg	105.54(1)	107.96(2)	109.79(2)		96.545(9)
γ, deg	92.01(1)	78.28(2)	80.78(2)		94.81(1)
cell vol, Å ³	1748.1(6)	1770.3(6)	1914.1(7)	2895(2)	2112.0(4)
Z	2	2	2	4	2
D _{measd} , ^a g cm ⁻³	nd ^b	1.48	nd ^b	1.54	1.56
D _{calcd} , g cm ⁻³	1.423	1.484	1.397	1.539	1.560
F(000), e	776	816	836	1376	1008
μ(Mo Kα), cm ⁻¹	9.87	9.83	9.36	10.54	9.87
cryst dimens, mm	0.28 × 0.10 × 0.72	0.35 × 0.15 × 0.68	0.20 × 0.15 × 0.20	0.38 × 0.20 × 0.16	0.24 × 0.31 × 0.62
(B) Data Collection					
diffractometer	Rigaku AFC7R	MAC MXC-18	Rigaku AFC7R	Rigaku AFC5S	Rigaku AFC7R
monochromator			graphite		
radiation (λ, Å)			Mo Kα (0.7107)		
temp			room temp		
2θ _{max} , deg	55	50	50	55	55
scan method			ω-2θ		
scan speed, deg min ⁻¹			16		
rflns measd	+h,±k,±l	+h,±k,±l	+h,±k,±l	+h,+k,+l	+h,±k,±l
no. of unique rflns	8017	6317	6752	3750	9690
abs cor	ψ-scan method	Gaussian integration	ψ-scan method	ψ-scan method	ψ-scan method
transmissn factors	0.76–1.00		0.94–1.00	0.91–1.00	0.75–1.00
(C) Solution and Refinement					
no. of observns	5596 (I > 3σ(I))	5448 (F _o > 3σ(F _o))	2352 (I > 3σ(I))	1956 (I > 3σ(I))	5103 (I > 3σ(I))
no. of variables	352	380	204	327	478
R	0.051	0.045	0.079	0.049	0.068
R _w	0.058	0.057	0.051	0.036	0.088
max resid density, e Å ⁻³	0.75	0.67	0.99	0.61	0.93

^a Flotation. ^b nd = not determined.

F₅)₂Mn(CO)₄, but this afforded the monomeric metallathiacyclobutene complex(OC)₄Mn[C(CF₃)=C(CF₃)SC₆F₅].^{14g}

X-ray Crystal Structure of 5c. The molecular structure of 5c is shown in Figure 1, and relevant crystallographic parameters are given in Tables 1–3. Figure 1 clearly indicates the dinuclear metallacyclic structure of 5c formed by the insertion of HC≡CCO₂Bu^t into one of the Ru–S bonds in 1 accompanied by ring closure. The Ru–Ru single bond (2.747(1) Å) is bridged by both one SPrⁱ group and the vinyl ligand, the latter being σ-bonded to Ru(1) (Ru(1)–C(1) = 2.149(8) Å) and π-bonded to Ru(2) (Ru(2)–C(1) = 2.033(8) Å, Ru(2)–C(2) = 2.143(8) Å). The sulfur atom in the SPrⁱ group attached to the β-carbon of the vinyl ligand coordinates to Ru(1) (Ru(1)–S(1) = 2.429(2) Å), forming the four-membered metallacycle. The SPrⁱ and CO₂Bu^t substituents on the vinyl ligand, having a relatively long C=C distance (C(1)–C(2) = 1.45(1) Å), adopt a “bent back” conformation with a dihedral angle of 124.2(8)° between the S(1)–C(2)–C(1) and C(2)–C(1)–C(3) planes. These structural features are in good accordance with

those observed for the related dinuclear complexes having a four-membered MC₂P ring.¹⁷

Reactions of 5a with HC≡CR' (R' = CO₂Me, Tol)

To Form Dinuclear Ruthenacyclopentenyl Complexes 6. In contrast to the formation of 5a from the reaction of 1 with 1 equiv of HC≡CCO₂Me, treatment of 1 with HC≡CCO₂Me (5 equiv) at room temperature afforded the diruthenium complex Cp^{*}Ru(μ₂-SPrⁱ)[η²:η³-μ₂-C(CO₂Me)CHC(CO₂Me)CHSPri]RuCp^{*} (**6a**), containing a new type of ruthenacyclopentenyl core derived from the coupling of two alkyne molecules and concurrent ring closure. Complex **6a** has also been obtained in moderate yield upon treatment of the isolated **5a** with HC≡CCO₂Me (2.6 equiv) at 50 °C, demonstrating that **5a** represents the intermediate for the formation of the dinuclear ruthenacyclopentenyl complex **6a** from 1 (Scheme 2). An X-ray analysis has been carried out to clarify the detailed structure of **6a**, the result of which is depicted in Figure 2. The IR spectrum shows two ν-(C=O) bands at 1686 and 1715 cm⁻¹, indicating the presence of two CO₂Me groups, while the ¹H NMR spectrum exhibits two doublets at δ 2.99 and 5.51 mutually coupled with ⁴J_{HH} = 1.2 Hz, assignable to the two methine protons attached to C(7) and C(11) in the ruthenacyclopentenyl moiety. Other spectroscopic data for **6a** are also consistent with this structure. It has

(16) (a) Seyferth, D.; Anderson, L. L.; Davis, W. B.; Cowie, M. *Organometallics* **1992**, *11*, 3736. (b) Rumin, R.; Petillon, F.; Manojlović-Muir, Lj.; Muir, K. W. *Organometallics* **1990**, *9*, 944. (c) Fässler, Th.; Huttner, G. J. *Organomet. Chem.* **1990**, *381*, 391. (d) Schrauzer, G. N.; Rabinowitz, H. N.; Frank, J. A. K.; Paul, I. C. *J. Am. Chem. Soc.* **1970**, *92*, 212.

(17) (a) Martín, A.; Mays, M. J.; Raithby, P. R.; Solan, G. A. *J. Chem. Soc., Dalton Trans.* **1993**, 1431. (b) Conole, G.; Hill, K. A.; McPartlin, M.; Mays, M. J.; Morris, M. J. *J. Chem. Soc., Chem. Commun.* **1989**, 688.

Table 2. Atomic Coordinates for **5c**^a

	x	y	z	B _{eq} , Å ²
Ru(1)	0.33763(7)	-0.22395(5)	0.17020(9)	2.38(2)
Ru(2)	0.12097(6)	-0.20608(5)	0.25112(9)	2.26(2)
S(1)	0.4112(2)	-0.2405(1)	0.4484(3)	2.55(5)
S(2)	0.2431(2)	-0.1112(1)	0.2019(3)	2.94(6)
O(1)	0.1612(6)	-0.4103(4)	0.1297(8)	4.5(2)
O(2)	0.2313(6)	-0.4062(4)	0.3847(8)	3.9(2)
C(1)	0.2340(7)	-0.2932(5)	0.281(1)	2.2(2)
C(2)	0.2599(7)	-0.2499(5)	0.4285(10)	2.2(2)
C(3)	0.2038(8)	-0.3748(5)	0.252(1)	2.8(2)
C(4)	0.219(1)	-0.4903(6)	0.390(2)	5.3(4)
C(5)	0.305(1)	-0.5264(6)	0.300(2)	6.9(4)
C(6)	0.262(1)	-0.4972(7)	0.561(2)	7.3(4)
C(7)	0.084(1)	-0.5199(6)	0.318(2)	5.9(4)
C(8)	0.5159(8)	-0.2792(5)	0.528(1)	3.1(2)
C(9)	0.6484(9)	-0.2421(7)	0.563(1)	5.3(3)
C(10)	0.4889(10)	-0.3013(7)	0.674(1)	5.3(3)
C(11)	0.3413(9)	-0.0413(5)	0.357(1)	3.8(3)
C(12)	0.361(1)	0.0280(6)	0.276(2)	7.4(4)
C(13)	0.276(1)	-0.0246(7)	0.483(1)	6.5(4)
C(14)	0.337(1)	-0.1994(7)	-0.065(1)	4.4(3)
C(15)	0.2985(9)	-0.2777(7)	-0.069(1)	3.9(3)
C(16)	0.400(1)	-0.3157(7)	0.022(1)	4.2(3)
C(17)	0.498(1)	-0.2611(9)	0.084(1)	5.9(4)
C(18)	0.462(1)	-0.1865(8)	0.032(1)	5.2(4)
C(19)	0.266(1)	-0.1397(8)	-0.158(1)	7.4(4)
C(20)	0.1782(10)	-0.3158(7)	-0.169(1)	5.9(3)
C(21)	0.411(1)	-0.3984(7)	0.032(2)	6.9(4)
C(22)	0.632(1)	-0.281(1)	0.713(2)	10.3(5)
C(23)	0.552(1)	-0.1159(8)	0.062(2)	9.6(5)
C(24)	-0.0496(8)	-0.1345(7)	0.206(1)	4.3(3)
C(25)	-0.0392(7)	-0.1765(6)	0.342(1)	3.7(3)
C(26)	-0.0470(8)	-0.2571(6)	0.286(1)	3.6(3)
C(27)	-0.0618(8)	-0.2653(6)	0.127(1)	4.0(3)
C(28)	-0.0619(8)	-0.1918(9)	0.075(1)	5.2(3)
C(29)	-0.055(1)	-0.0504(6)	0.202(2)	7.0(4)
C(30)	-0.0383(10)	-0.1426(7)	0.501(1)	6.0(3)
C(31)	-0.0554(10)	-0.3194(7)	0.388(2)	6.4(4)
C(32)	-0.092(1)	-0.3354(7)	0.015(2)	7.3(4)
C(33)	-0.080(1)	-0.1680(9)	-0.090(1)	8.4(5)

^a Numbers in parentheses are estimated standard deviations.Table 3. Selected Bond Distances and Angles for **5c**^a

Distances (Å)			
Ru(1)–Ru(2)	2.747(1)	Ru(1)–S(1)	2.429(2)
Ru(1)–S(2)	2.343(3)	Ru(1)–C(1)	2.149(8)
Ru(1)–C(14)	2.212(10)	Ru(1)–C(15)	2.227(10)
Ru(1)–C(16)	2.28(1)	Ru(1)–C(17)	2.25(1)
Ru(1)–C(18)	2.23(1)	Ru(2)–S(2)	2.291(3)
Ru(2)–C(1)	2.033(8)	Ru(2)–C(2)	2.143(8)
Ru(2)–C(24)	2.306(9)	Ru(2)–C(25)	2.234(9)
Ru(2)–C(26)	2.178(9)	Ru(2)–C(27)	2.240(9)
Ru(2)–C(28)	2.277(10)	S(1)–C(2)	1.816(8)
S(1)–C(8)	1.871(9)	S(2)–C(11)	1.882(9)
C(1)–C(2)	1.45(1)		
Angles (deg)			
Ru(2)–Ru(1)–S(2)	52.79(6)	S(1)–Ru(1)–C(1)	67.7(2)
Ru(1)–Ru(2)–S(2)	54.53(7)	C(1)–Ru(2)–C(2)	40.4(3)
Ru(1)–S(1)–C(2)	80.4(3)	Ru(1)–S(2)–Ru(2)	72.68(8)
Ru(1)–C(1)–Ru(2)	82.0(3)	Ru(1)–C(1)–C(2)	99.4(6)
Ru(1)–C(1)–C(3)	128.6(6)	Ru(2)–C(1)–C(2)	73.8(5)
Ru(2)–C(1)–C(3)	130.1(6)	C(2)–C(1)–C(3)	125.3(8)
Ru(2)–C(2)–S(1)	111.2(4)	Ru(2)–C(2)–C(1)	65.7(5)
S(1)–C(2)–C(1)	102.8(6)		

^a Numbers in parentheses are estimated standard deviations.

also been found that $\text{HC}\equiv\text{CTol}$ reacts with **5a** analogously to $\text{HC}\equiv\text{CCO}_2\text{Me}$, affording the corresponding dinuclear ruthenacyclopentenyl complex $\text{Cp}^*\text{Ru}(\mu_2\text{-SPr}^i)[\eta^2\text{-}\eta^3\text{-}\mu_2\text{-C(Tol)}\text{CHC}(\text{CO}_2\text{Me})\text{CHSPr}^i]\text{RuCp}^*$ (**6b**), whose spectral data are diagnostic of the structure shown in Scheme 2.

X-ray Crystal Structure of **6a.** The molecular structure of **6a** is shown in Figure 2, and relevant

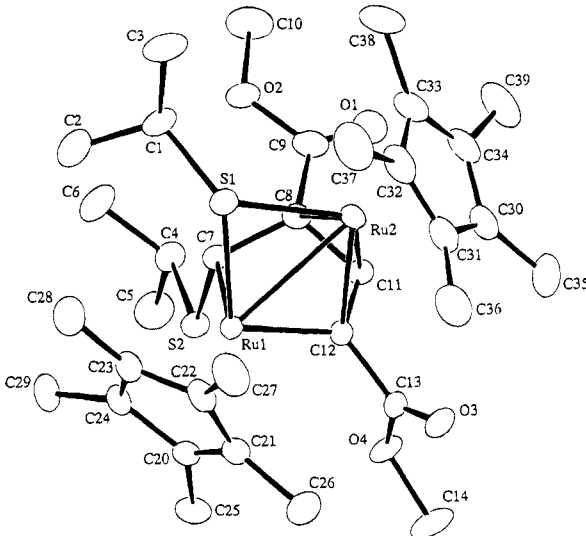


Figure 2. Molecular structure of **6a**, showing the atom-labeling scheme. The thermal ellipsoids are drawn at the 30% probability level.

Table 4. Atomic Coordinates for **6a**^a

	x	y	z	B _{eq} , Å ²
Ru(1)	0.85395(5)	0.19277(3)	0.32670(6)	1.9
Ru(2)	0.80917(5)	0.32834(3)	0.24771(6)	2.3
S(1)	0.7189(2)	0.2896(10)	0.4110(2)	2.8
S(2)	0.7177(2)	0.1038(10)	-0.0076(2)	2.7
O(1)	0.5928(5)	0.3169(3)	-0.1633(6)	4.4
O(2)	0.4720(4)	0.2825(3)	-0.0412(6)	3.7
O(3)	1.1420(4)	0.2436(3)	0.2382(6)	3.9
O(4)	1.0679(4)	0.1531(3)	0.0533(6)	3.6
C(1)	0.5404(8)	0.2887(5)	0.3426(10)	4.0
C(2)	0.5053(10)	0.2248(6)	0.3872(13)	5.5
C(3)	0.4794(10)	0.3604(6)	0.4290(13)	6.1
C(4)	0.5649(7)	0.1020(4)	-0.1628(8)	3.0
C(5)	0.5811(9)	0.0324(5)	-0.2790(10)	4.7
C(6)	0.4499(8)	0.1042(6)	-0.1005(11)	4.7
C(7)	0.6932(6)	0.1888(4)	0.1210(7)	2.3
C(8)	0.6972(7)	0.2530(4)	0.0502(8)	2.5
C(9)	0.5874(8)	0.2878(4)	-0.0633(9)	3.4
C(10)	0.3571(10)	0.3140(7)	-0.1501(15)	7.1
C(11)	0.8230(7)	0.2536(4)	0.0411(8)	2.4
C(12)	0.9173(6)	0.2262(3)	0.1687(8)	2.2
C(13)	1.0549(7)	0.2113(4)	0.1623(9)	3.0
C(14)	1.1988(9)	0.1297(7)	0.0356(13)	6.3
C(20)	0.9755(7)	0.0857(4)	0.3582(8)	2.8
C(21)	1.0496(7)	0.1397(4)	0.4600(9)	3.2
C(22)	0.9818(8)	0.1772(4)	0.5701(8)	3.3
C(23)	0.8700(7)	0.1442(4)	0.5434(8)	3.0
C(24)	0.8630(7)	0.0893(4)	0.4132(8)	2.9
C(25)	1.0167(9)	0.0267(4)	0.2359(10)	4.0
C(26)	1.1874(8)	0.1457(6)	0.4706(12)	5.1
C(27)	1.0237(10)	0.2371(5)	0.7055(10)	5.0
C(28)	0.7843(10)	0.1611(6)	0.6505(10)	4.5
C(29)	0.7682(9)	0.0353(4)	0.3513(10)	4.0
C(30)	0.9336(9)	0.4031(4)	0.2205(10)	3.8
C(31)	0.9586(9)	0.4021(4)	0.3838(10)	3.9
C(32)	0.8413(10)	0.4291(4)	0.4240(10)	4.4
C(33)	0.7401(9)	0.4472(4)	0.2838(11)	4.5
C(34)	0.8012(10)	0.4300(4)	0.1588(11)	4.4
C(35)	1.0299(11)	0.3888(6)	0.1279(13)	5.7
C(36)	1.0889(10)	0.3832(6)	0.4968(12)	5.5
C(37)	0.8244(13)	0.4446(6)	0.5880(11)	6.2
C(38)	0.6032(12)	0.4865(6)	0.2761(16)	7.3
C(39)	0.7382(12)	0.4488(6)	-0.0029(12)	6.4

^a Numbers in parentheses are estimated standard deviations.

crystallographic data are given in Tables 1, 4, and 5, respectively. Complex **6a** has a dinuclear structure where two Cp^*Ru units are bridged by one SPr^i group and the $\eta^2\text{-}\eta^3\text{-}\mu_2\text{-C}(\text{CO}_2\text{Me})\text{CHC}(\text{CO}_2\text{Me})\text{CHSPr}^i$ moiety,

Table 5. Selected Bond Distances and Angles for $6\alpha^*$

	Distances (\AA)	
	Ru(1)–Ru(2)	Ru(1)–S(1)
Ru(1)–C(7)	2.750(1)	2.285(2)
Ru(1)–C(20)	2.147(6)	2.043(8)
Ru(1)–C(22)	2.230(7)	2.273(7)
Ru(1)–C(24)	2.280(7)	2.306(9)
Ru(1)–C(26)	2.257(8)	2.333(2)
Ru(2)–C(8)	2.259(6)	2.142(6)
Ru(2)–C(12)	2.180(6)	2.268(10)
Ru(2)–C(31)	2.277(9)	2.249(8)
Ru(2)–C(33)	2.238(8)	2.239(10)
S(1)–C(1)	1.871(8)	1.836(7)
S(2)–C(7)	1.820(6)	1.52(1)
C(8)–C(11)	1.41(1)	1.415(9)

	Angles (deg)		
Ru(2)–Ru(1)–S(1)	54.27(6)	Ru(2)–Ru(1)–C(7)	75.8(2)
Ru(2)–Ru(1)–C(12)	49.8(2)	C(7)–Ru(1)–C(12)	76.3(3)
Ru(1)–Ru(2)–S(1)	52.64(5)	Ru(1)–Ru(2)–C(12)	50.2(2)
C(8)–Ru(2)–C(11)	37.4(3)	C(8)–Ru(2)–C(12)	63.2(2)
C(11)–Ru(2)–C(12)	38.2(2)	Ru(1)–S(1)–Ru(2)	73.09(7)
Ru(1)–C(7)–C(8)	103.3(4)	Ru(2)–C(8)–C(7)	105.7(4)
Ru(2)–C(8)–C(11)	66.8(4)	C(7)–C(8)–C(11)	111.1(6)
Ru(2)–C(11)–C(8)	75.8(4)	Ru(2)–C(11)–C(12)	72.4(4)
C(8)–C(11)–C(12)	110.6(7)	Ru(1)–C(12)–Ru(2)	81.2(3)
Ru(1)–C(12)–C(11)	117.7(5)	Ru(2)–C(12)–C(11)	69.4(4)

^a Numbers in parentheses are estimated standard deviations.

the latter of which is derived from the (isopropylthio)-alkenyl ligand in **5a** and one $\text{HC}\equiv\text{CCO}_2\text{Me}$ molecule. The two alkyne molecules on the diruthenium site are combined in a head-to-tail manner, generating a five-membered metallacycle with Ru(1), a part of which (C(8), C(11), and C(12)) coordinates to Ru(2) via a η^3 -allyl linkage. The S(2)–Prⁱ group and the Ru(2)–Cp* unit adopt an *anti* configuration with respect to the metallacycle. The Ru(1)–Ru(2) distance of 2.750(1) Å corresponds to a Ru–Ru single bond.

Reaction of **5a with $\text{HC}\equiv\text{CSiMe}_3$ To Form Diruthenium Bridging Alkyne Complex **7**.** In sharp contrast to the formation of the dinuclear ruthenacyclopentenyl complexes **6** described above, reaction of **5a** with $\text{HC}\equiv\text{CSiMe}_3$ proceeded in quite a different manner and the product has been spectroscopically and crystallographically characterized to be the bridging alkyne complex $\text{Cp}^*\text{Ru}(\mu_2\text{-SPri})(\mu_2\text{-H})[\eta^2\text{-}\eta^2\text{-}\mu_2\text{-Me}_3\text{SiC}\equiv\text{CC}(\text{CO}_2\text{Me})=\text{CHSPri}] \text{RuCp}^*$ (**7**) (Scheme 2). The IR (KBr) spectrum of **7** shows the characteristic $\nu(\text{C=O})$ and $\nu(\text{C=C})$ bands at 1686 and 1607 cm⁻¹, respectively. The ¹H NMR spectrum of **7** ($\text{C}_6\text{D}_5\text{CD}_3$) indicates the presence of two types of isomers in *ca.* 2:1 ratio in the solution at 22 °C (see Experimental Section). Each isomer shows only one Cp* resonance, which implies the two Cp* ligands are in equivalent environments for both isomers. As the temperature is raised, the resonances of the Cp* ligands began to broaden at around 80 °C, but at temperatures higher than 80 °C thermal decomposition of **7** occurred. Considering the crystal structure of **7** described below, these observations may presumably be attributed to the presence of two conformational isomers, **7-I** and **7-II**, arising from a restricted rotation of

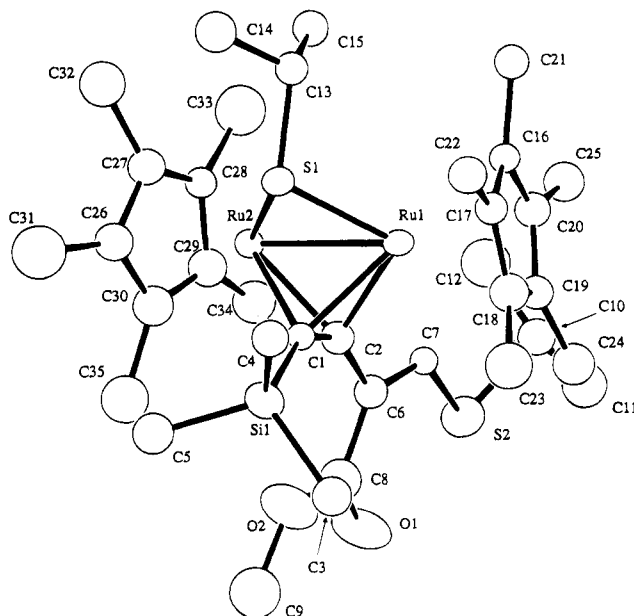
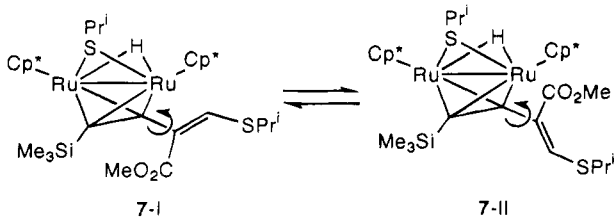


Figure 3. Molecular structure of **7**, showing the atom-labeling scheme. The thermal ellipsoids are drawn at the 50% probability level.

Table 6. Atomic Coordinates for **7**^a

	x	y	z	$B_{eq}, \text{\AA}^2$
Ru(1)	0.2051(2)	0.1978(5)	0.1441(2)	2.29(7)
Ru(2)	0.2718(2)	0.3470(1)	0.2161(2)	2.27(7)
S(1)	0.0622(6)	0.3122(3)	0.1204(6)	2.9(2)
S(2)	0.7072(6)	0.1487(4)	0.3234(7)	4.9(2)
Si(1)	0.1877(7)	0.2749(4)	-0.1618(7)	3.8(2)
O(1)	0.675(2)	0.206(1)	0.087(2)	8.0(7)
O(2)	0.502(2)	0.260(1)	-0.043(2)	6.7(6)
C(1)	0.255(2)	0.268(1)	0.023(2)	2.0(5)
C(2)	0.353(2)	0.246(1)	0.118(2)	3.0(5)
C(3)	0.259(2)	0.191(1)	-0.271(2)	4.3(6)
C(4)	0.009(2)	0.266(1)	-0.227(2)	3.7(6)
C(5)	0.212(2)	0.373(1)	-0.193(2)	4.6(6)
C(6)	0.492(2)	0.215(1)	0.157(2)	3.1(6)
C(7)	0.549(2)	0.182(1)	0.269(2)	2.1(5)
C(8)	0.559(3)	0.226(2)	0.061(3)	4.8(7)
C(9)	0.576(3)	0.275(2)	-0.130(3)	7.1(8)
C(10)	0.711(2)	0.105(1)	0.473(2)	3.7(6)
C(11)	0.850(2)	0.064(1)	0.522(2)	5.4(7)
C(12)	0.684(2)	0.171(1)	0.586(2)	6.4(8)
C(13)	-0.033(2)	0.322(1)	0.236(2)	3.0(5)
C(14)	-0.134(2)	0.391(1)	0.206(2)	4.5(6)
C(15)	0.047(2)	0.326(1)	0.390(2)	3.5(6)
C(16)	0.121(2)	0.114(1)	0.216(2)	2.5(5)
C(17)	0.073(2)	0.105(1)	0.072(2)	2.8(5)
C(18)	0.176(2)	0.076(1)	0.017(2)	4.1(6)
C(19)	0.285(2)	0.065(1)	0.127(2)	3.1(5)
C(20)	0.256(2)	0.089(1)	0.252(2)	3.4(5)
C(21)	0.041(2)	0.127(1)	0.315(2)	3.1(5)
C(22)	-0.072(2)	0.119(1)	-0.011(2)	4.0(6)
C(23)	0.162(2)	0.053(1)	-0.134(3)	5.8(7)
C(24)	0.409(2)	0.024(1)	0.116(2)	4.7(6)
C(25)	0.348(2)	0.080(1)	0.397(2)	4.4(6)
C(26)	0.272(2)	0.474(1)	0.225(2)	3.9(6)
C(27)	0.250(2)	0.464(1)	0.344(2)	3.8(6)
C(28)	0.355(2)	0.422(1)	0.416(2)	2.7(5)
C(29)	0.450(2)	0.402(1)	0.353(2)	4.0(6)
C(30)	0.399(2)	0.435(1)	0.233(2)	4.5(7)
C(31)	0.190(3)	0.531(2)	0.127(3)	7.9(9)
C(32)	0.139(2)	0.516(1)	0.389(2)	5.5(7)
C(33)	0.363(3)	0.408(2)	0.560(3)	6.8(8)
C(34)	0.578(2)	0.364(1)	0.416(2)	5.0(7)
C(35)	0.466(2)	0.442(2)	0.128(2)	6.0(7)

^a Numbers in parentheses are estimated standard deviations.

the $\text{C}(\text{CO}_2\text{Me})=\text{CHSPri}$ group around the C(2)–C(6) bond due to the steric requirement of a large Cp* ligand.

Table 7. Selected Bond Distances and Angles for **7^a**

Distances (Å)			
Ru(1)–Ru(2)	2.698(3)	Ru(1)–S(1)	2.350(6)
Ru(1)–C(1)	2.19(2)	Ru(1)–C(2)	2.10(2)
Ru(1)–C(16)	2.23(2)	Ru(1)–C(17)	2.22(2)
Ru(1)–C(18)	2.27(2)	Ru(1)–C(19)	2.34(2)
Ru(1)–C(20)	2.30(2)	Ru(2)–S(1)	2.367(6)
Ru(2)–C(1)	2.19(2)	Ru(2)–C(2)	2.10(2)
Ru(2)–C(26)	2.19(2)	Ru(2)–C(27)	2.23(2)
Ru(2)–C(28)	2.24(2)	Ru(2)–C(29)	2.27(2)
Ru(2)–C(30)	2.20(2)	S(1)–C(13)	1.86(2)
S(2)–C(7)	1.73(2)	S(2)–C(10)	1.88(2)
Si(1)–C(1)	1.88(2)	C(1)–C(2)	1.30(3)
C(2)–C(6)	1.52(3)	C(6)–C(7)	1.35(2)

Angles (deg)			
Ru(2)–Ru(1)–S(1)	55.4(2)	Ru(2)–Ru(1)–C(1)	51.9(5)
Ru(2)–Ru(1)–C(2)	50.0(6)	S(1)–Ru(1)–C(1)	71.6(5)
S(1)–Ru(1)–C(2)	96.2(6)	C(1)–Ru(1)–C(2)	35.0(7)
Ru(1)–Ru(2)–S(1)	54.8(2)	Ru(1)–Ru(2)–C(1)	52.0(5)
Ru(1)–Ru(2)–C(2)	50.1(6)	S(1)–Ru(2)–C(1)	71.3(5)
S(1)–Ru(2)–C(2)	95.8(6)	C(1)–Ru(2)–C(2)	35.1(7)
Ru(1)–C(1)–Ru(2)	76.1(6)	Ru(1)–C(1)–C(2)	68(1)
Ru(2)–C(1)–C(2)	68(1)	Si(1)–C(1)–C(2)	145(1)
Ru(1)–C(2)–Ru(2)	79.8(7)	Ru(1)–C(2)–C(1)	76(1)
Ru(2)–C(2)–C(1)	76(1)	C(1)–C(2)–C(6)	145(2)

^a Numbers in parentheses are estimated standard deviations.

ligand.¹⁸ The ¹H NMR spectrum also displays two singlets assignable to the hydride ligands in two isomers. Since a symmetrical structure is suggested for both isomers of **7** (see above), the hydride ligand probably bridges the Ru–Ru bond.

X-ray Crystal Structure of **7.** The molecular structure is depicted in Figure 3, and related crystallographic parameters are listed in Tables 1, 6, and 7. Figure 3 clearly shows that coupling of a (trimethylsilyl)ethynyl unit with the isopropylthioalkenyl ligand forms the $\eta^2:\eta^2$ -Me₃SiC≡CC(CO₂Me)=CHSPri moiety, which perpendicularly bridges the Ru–Ru single bond (Ru(1)–Ru(2) = 2.698(3) Å). The relative position of the SPri and CO₂Me groups changed from mutually *trans* (in **5a**) to mutually *cis* (in **7**) in this transformation. Although the hydrogen atom attached to Ru was not located by the X-ray structural analysis, the existence of a μ_2 -hydride ligand is strongly suggested by the large dihedral angle of 221.38° between the two planes defined by the two Ru and S(1) atoms and the two Ru and C(2) atoms. The C(1)–C(2) distance at 1.30(3) Å is comparable to those of π -bound alkyne ligands in the

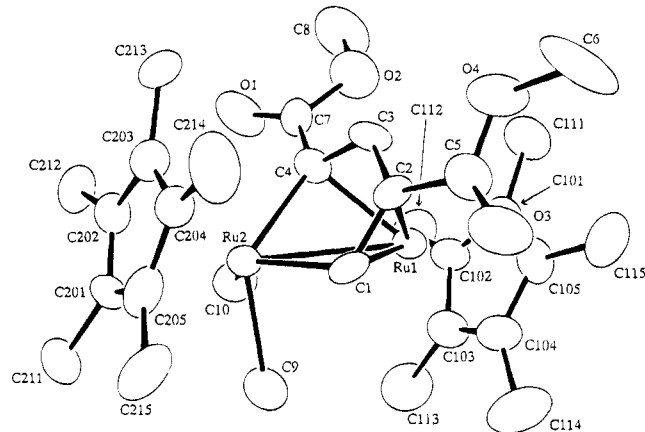


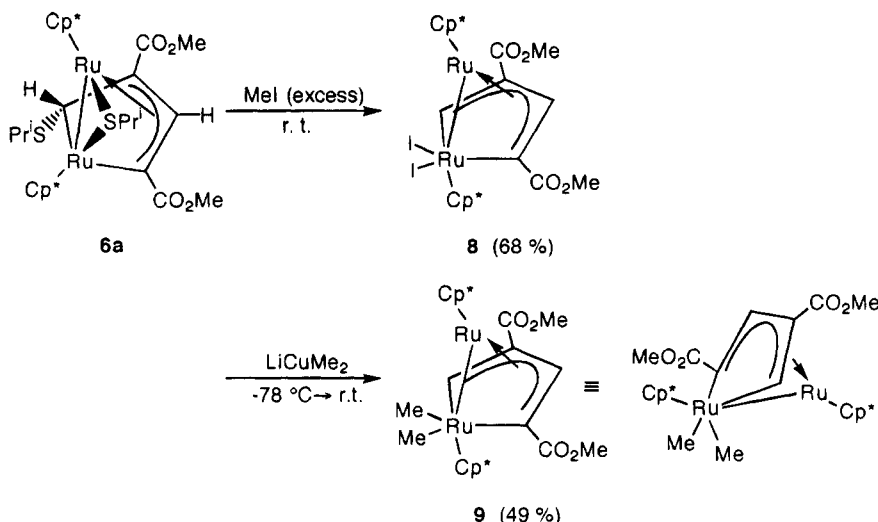
Figure 4. Molecular structure of **9**, showing the atom-labeling scheme. The thermal ellipsoids are drawn at the 50% probability level.

diruthenium complexes Cp*Ru(μ_2 -H)(μ_2 -SPri)[$\eta^2:\eta^2$ -Me₃SiC≡CC(C=CSiMe₃)=CHSiMe₃]RuCp* (1.316(9) Å),^{8a} Cp*Ru(μ_2 -H)₂($\eta^2:\eta^2$ - μ_2 -PhC≡CPh)RuCp* (1.315(8) Å),¹⁹ and CpRu(μ_2 -CO)($\eta^2:\eta^2$ - μ_2 -PhC≡CPh)RuCp (1.336(12) Å).²⁰ The Ru–C(acetylenic) distance of 2.15 Å (average) is within the normal range of that in ruthenium π -alkyne complexes.²¹

Conversion of Dinuclear Ruthenacyclopentenyl Complexes **6 to Dinuclear Ruthenacyclopentadiene Complexes.** Complex **6a** reacted with excess MeI to afford the neutral diiodo ruthenacyclopentadiene complex Cp*I₂Ru[$\eta^2:\eta^4$ - μ_2 -C(CO₂Me)CHC(CO₂Me)CH]RuCp* (**8**) as reddish brown crystals (Scheme 3). Both SPri groups in **6a** have been removed from the dinuclear site. The ¹H NMR spectrum of **8** exhibits two doublets at δ 9.73 and 6.10 with a $^4J_{HH}$ value of 1.8 Hz assignable to the α - and β -protons in the ruthenacyclopentadiene moiety, respectively, in addition to the Cp* (δ 1.86 and 1.60) and CO₂Me (δ 3.60 and 3.51) resonances. These ¹H NMR data correspond well with those of the related dinuclear ruthenacyclopentadiene complexes Cp*Cl₂Ru[$\eta^2:\eta^4$ - μ_2 -C(R²)CHC(R²)CH]RuCp* (R² = H, SiMe₃) previously reported by Tilley and co-workers.²²

The structure of **8** has been further confirmed by X-ray crystallography of its dimethyl derivative Cp*Me₂Ru[$\eta^2:\eta^4$ - μ_2 -C(CO₂Me)CHC(CO₂Me)CH]RuCp* (**9**) (Figure 4), which was isolated as an orange microcrystalline

Scheme 3



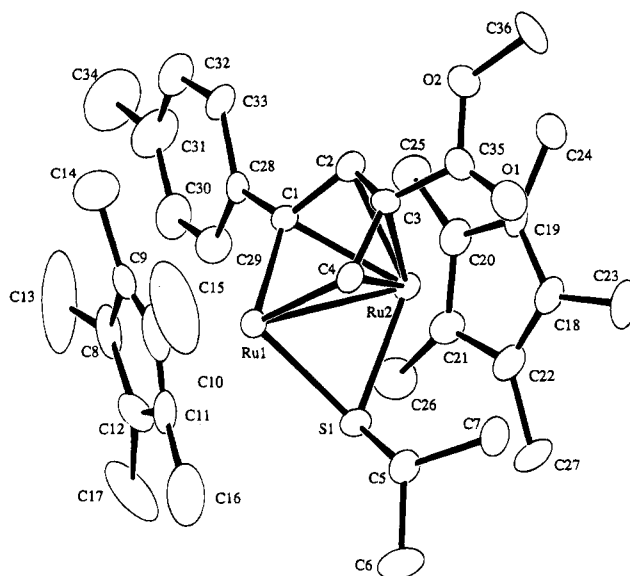
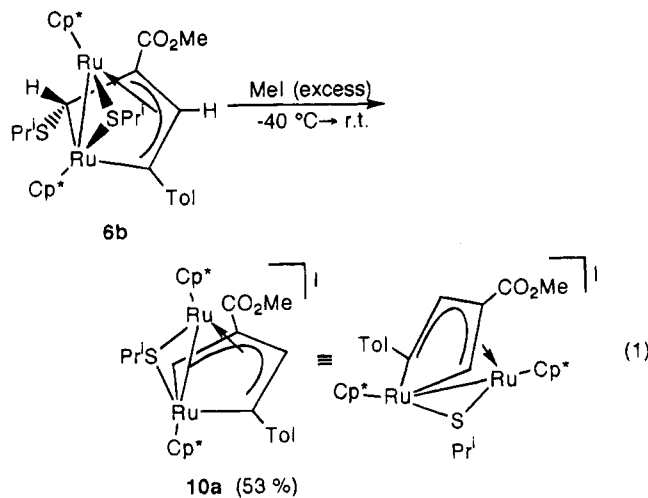


Figure 5. Molecular structure of the cation in $10\mathbf{b}\cdot\text{ClCH}_2\text{-CH}_2\text{Cl}$, showing the atom-labeling scheme. The thermal ellipsoids are drawn at the 30% probability level.

solid from the reaction of **8** with an equimolar amount of LiCuMe_2 (Scheme 3). The spectroscopic data for **9** are essentially similar to those for **8**, except for the appearance of the $\text{Ru}-\text{CH}_3$ resonances in the ^1H NMR spectrum of **9** at δ 0.55 and 0.54.

On the other hand, treatment of **6b** with MeI at -40°C gives another type of dinuclear ruthenacyclopentadiene complex, $[\text{Cp}^*\text{Ru}(\mu_2\text{-SPri})\{\eta^2\text{-}\mu_2\text{-C(Tol)}\text{CHC}(\text{CO}_2\text{Me})\text{CH}\}\text{RuCp}^*]\text{I}$ (**10a**) (eq 1). The X-ray structure



of this cationic complex **10a** has been determined by using a single crystal of **10b** obtained after the anion metathesis of **10a** by PF_6^- (Figure 5). In the present reaction, the bridging SPri ligand is intact and only the SPri group in the five-membered metallacycle in **6b** has been removed. The ^1H NMR spectrum of **10b** (CDCl_3) exhibits one singlet at δ 1.49 attributed to Cp^* ligands

(18) In contrast, the ^1H NMR spectrum of the closely related diruthenium alkyne complex **2** at room temperature exhibited only one set of signals, indicating the presence of a single isomer. This may be attributed to the bulkier substituent on the bridging alkyne ligand in **2**, which prevents a rotation around the corresponding carbon–carbon single bond.

(19) Omori, H.; Suzuki, H.; Kakigano, T.; Moro-oka, Y. *Organometallics* **1992**, *11*, 989.

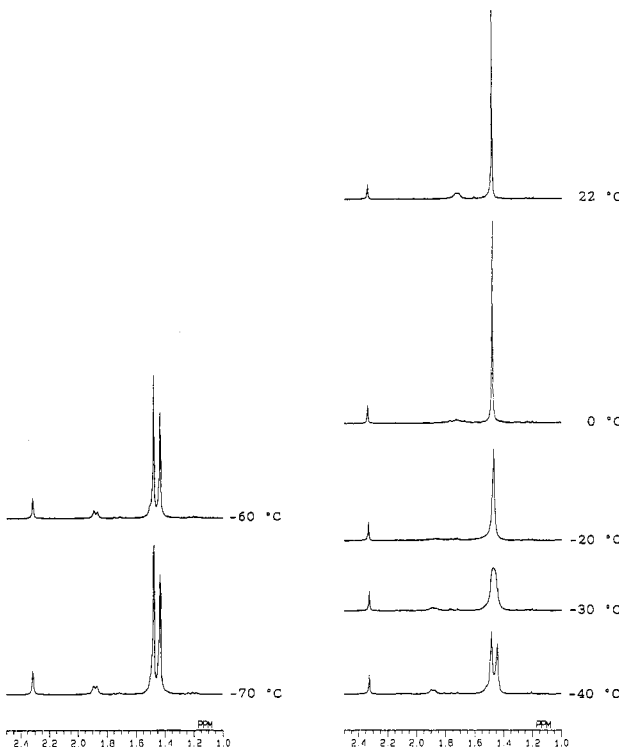
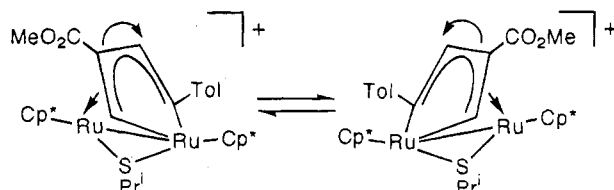


Figure 6. Variable-temperature ^1H NMR spectra of **10b** in the range δ 1–2.5 ppm (270 MHz, CDCl_3).

at room temperature. The variable-temperature ^1H NMR spectra of **10b** in the range of 1–2.5 ppm are shown in Figure 6. As the temperature is lowered, the Cp^* singlet broadened, coalesced at ca. -30°C , and then split into two singlets at δ 1.49 and 1.45 below -60°C . On the other hand, coalescence of the SPri methyl signal at δ 1.73 occurred at around 0°C . At lower temperatures it appeared as two doublets at δ 1.88 and 1.48, the latter of which overlapped with the Cp^* resonance. These spectroscopic features can be rationalized by the occurrence of the fluxional process depicted below:



Similar fluxional behavior has been observed for the dicobalt complex $\text{CpCo}(\eta^2\text{-}\mu_2\text{-C}_4\text{H}_4)\text{CoCp}$.²³

Scheme 4 shows the plausible reaction pathways for the transformations of **6a** and **6b** into **8** and **10a**, respectively. Both of these reactions presumably proceed via an initial electrophilic attack of MeI on the sulfur atom attached to the metallacycle, which results in the elimination of the SPri group from the metallacycle as MeSPri . Reactions of dialkyl sulfides with alkyl halides are known to proceed in a similar manner, which

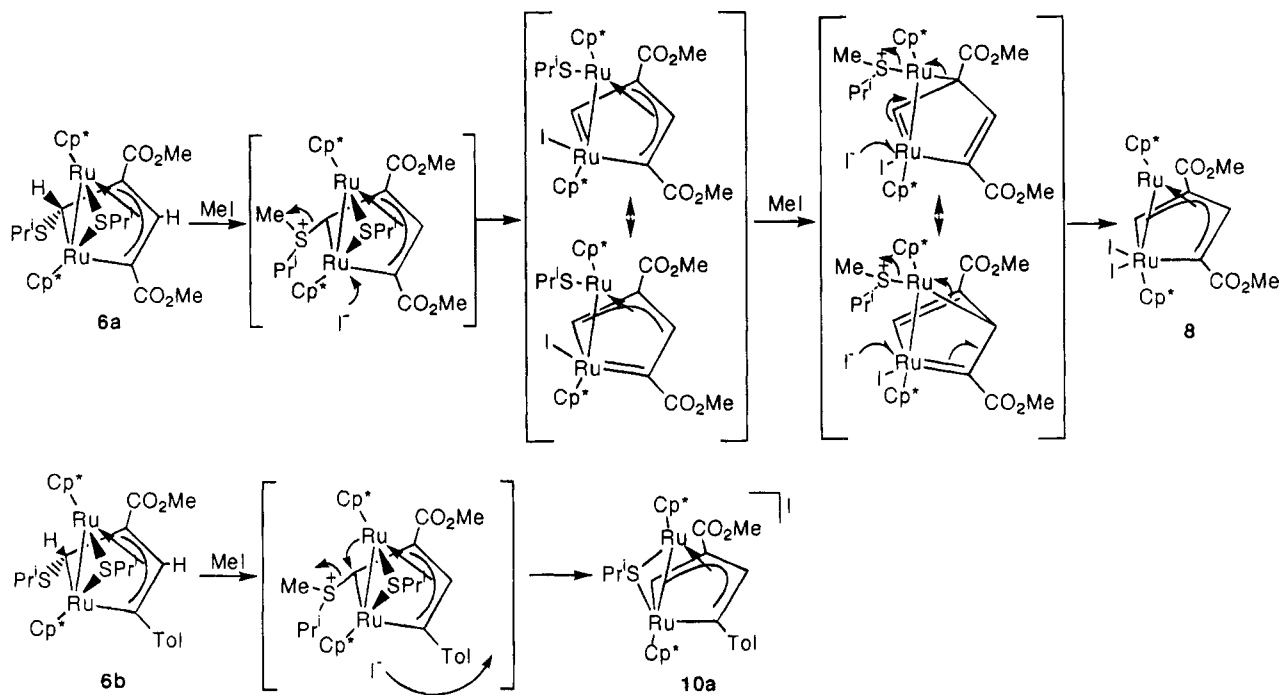
(20) Colborn, R. E.; Dyke, A. F.; Benjamin, P. G.; Knox, S. A. R.; Macpherson, K. A.; Mead, K. A.; Orpen, A. G. *J. Chem. Soc., Dalton Trans.* **1990**, 761.

(21) Hoffman, D. M.; Hoffmann, R.; Fisel, C. R. *J. Am. Chem. Soc.* **1982**, *104*, 3858 and references cited therein.

(22) Campion, B. K.; Heyn, R. H.; Tilley, T. D. *Organometallics* **1990**, *9*, 1106.

(23) Rosenblum, M.; North, B.; Wells, D.; Giering, W. P. *J. Am. Chem. Soc.* **1972**, *94*, 1239.

Scheme 4



give alternative dialkyl sulfides with a different substituent on the sulfur atom *via* transient formation of labile sulfonium halides.²⁴ Interestingly, diruthenium complexes **3** and **4** did not react with MeI even at 50 °C. These results are in good accordance with the lower reactivity of organic vinyl sulfides toward alkyl halides.

X-ray Crystal Structure of 9 and 10b-ClCH₂CH₂Cl
C1. Molecular structures are depicted in Figures 4 and 5, and pertinent crystallographic data are given in Tables 1 and 8–11. As shown in Figure 4, **9** possesses a dinuclear structure in which the two ruthenium atoms are bridged by the $\eta^2:\eta^4-\mu_2$ -C(CO₂Me)CHC(CO₂Me)CH fragment. Two Cp* ligands occupy a *trans* disposition with respect to the Ru–Ru single bond (2.819(1) Å). The C₄ fragment (C(1), C(2), C(3), C(4)), forming a ruthenacyclopentadiene ring with Ru(2), is bound to Ru(1) *via* η^4 coordination. In the ruthenacyclopentadiene unit, the four carbon atoms C(1)–C(4) are nearly coplanar (C(1)–C(2)–C(3)–C(4) torsion angle 1(2)°). However, the five-membered ring is slightly puckered^{22,25} with a dihedral angle of *ca.* 16° around the C(1)–C(4) vector. It should be noted that the metallacyclopentadiene core in the related dinuclear complexes is generally planar,²⁶ and the examples containing the folded five-membered ring are still limited; e.g., Cp(CO)Ru($\eta^2:\eta^4-\mu_2$ -C₄(CF₃)₄)-RuCp (23.1°),^{25a} Cp*Cl₂Ru($\eta^2:\eta^4-\mu_2$ -C₄H₄)RuCp* (20.5°),²² and Cp*(PMe₃)Ru($\eta^2:\eta^4-\mu_2$ -C₄H₄)RuCp* (18.3°).^{25c}

Figure 5 shows the molecular structure of the cation in **10b-ClCH₂CH₂Cl**. Complex **10b** also has a dinuclear ruthenacyclopentadiene structure. However, the four

Table 8. Atomic Coordinates for **9**^a

	x	y	z	B _{eq} , Å ²
Ru(1)	0.44870(6)	0.77342(7)	0.5456(1)	2.50(5)
Ru(2)	0.48959(6)	0.78029(7)	0.3605(1)	2.44(5)
O(1)	0.3394(6)	0.9384(6)	0.320(1)	5.7(6)
O(2)	0.2763(7)	0.8893(6)	0.484(1)	5.6(7)
O(3)	0.4107(6)	0.5420(5)	0.552(1)	4.9(6)
O(4)	0.2898(7)	0.5979(6)	0.553(1)	5.7(7)
C(1)	0.4739(9)	0.6854(8)	0.426(1)	3.3(7)
C(2)	0.3954(8)	0.6744(7)	0.468(1)	2.3(7)
C(3)	0.3441(7)	0.7436(7)	0.456(1)	2.7(7)
C(4)	0.3833(8)	0.8108(8)	0.404(1)	2.7(7)
C(5)	0.369(1)	0.5972(8)	0.530(1)	3.4(8)
C(6)	0.256(1)	0.527(1)	0.612(2)	9(1)
C(7)	0.334(1)	0.8860(9)	0.397(1)	3.2(8)
C(8)	0.227(1)	0.961(1)	0.485(2)	8(1)
C(9)	0.6140(8)	0.765(1)	0.368(1)	3.9(8)
C(10)	0.5261(9)	0.9014(8)	0.344(1)	4.4(8)
C(101)	0.406(1)	0.816(1)	0.749(1)	3.5(8)
C(102)	0.4616(8)	0.8725(8)	0.701(1)	3.3(7)
C(103)	0.541(1)	0.832(1)	0.694(2)	3.8(8)
C(104)	0.528(1)	0.752(1)	0.730(2)	4(1)
C(105)	0.446(1)	0.7416(8)	0.763(1)	3.2(7)
C(111)	0.316(1)	0.832(1)	0.778(1)	5(1)
C(112)	0.448(1)	0.9617(8)	0.682(2)	5.5(9)
C(113)	0.618(1)	0.876(1)	0.667(2)	6(1)
C(114)	0.596(1)	0.689(1)	0.741(2)	7(1)
C(115)	0.410(1)	0.667(1)	0.818(2)	6(1)
C(201)	0.5374(8)	0.784(1)	0.110(1)	2.9(7)
C(202)	0.4621(9)	0.8256(9)	0.108(1)	3.1(7)
C(203)	0.4015(9)	0.770(1)	0.137(1)	3.6(8)
C(204)	0.438(1)	0.694(1)	0.162(1)	3.4(8)
C(205)	0.522(1)	0.7035(8)	0.139(1)	3.6(8)
C(211)	0.617(1)	0.8194(9)	0.064(2)	4.8(9)
C(212)	0.448(1)	0.9098(7)	0.064(2)	4.3(7)
C(213)	0.3103(8)	0.781(1)	0.133(1)	4.7(8)
C(214)	0.394(1)	0.616(1)	0.182(2)	6(1)
C(215)	0.584(1)	0.6349(9)	0.140(1)	5(1)

^a Numbers in parentheses are estimated standard deviations.

C and one Ru atoms in the five-membered ring in **10b** (C(1)–C(4) and Ru(1)) are nearly coplanar, with deviations of less than 0.02 Å for the C atoms and 0.07 Å for the Ru(1) atom. Two Cp*Ru units are further connected by a Ru–Ru single bond (2.720(1) Å) and one bridging SPrⁱ group.

(24) Barret, G. C. In *Comprehensive Organic Chemistry*; Jones, D. N., Ed.; Pergamon Press: Oxford, U.K., 1979; Vol. 3, p 36.

(25) (a) Brady, L. A.; Dyke, A. F.; Stephanie, E. G.; Knox, S. A. R.; Irving, A.; Nicholls, S. A.; Orpen, A. G. *J. Chem. Soc., Dalton Trans.* **1993**, 487. (b) He, X. D.; Chaudret, B.; Dahan, F.; Huang, Y. S. *Organometallics* **1991**, *10*, 970. (c) Omori, H.; Suzuki, H.; Moro-Oka, Y. *Organometallics* **1989**, *8*, 1576.

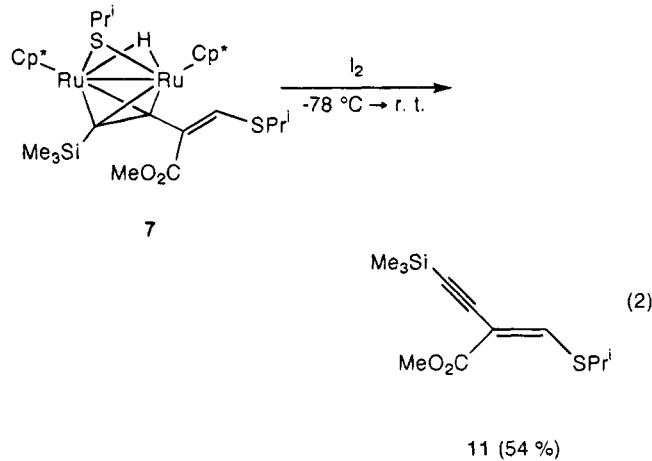
(26) Fehlhammer, W. P.; Stolzenberg, H. In *Comprehensive Organometallic Chemistry*; Wilkinson, G., Stone, F. G. A., Eds.; Pergamon Press: Oxford, U.K., 1982; Vol. 4, p 548.

Table 9. Selected Bond Distances and Angles for $\mathbf{9}^a$

	Distances (\AA)		
	Ru(1)–Ru(2)	Ru(1)–C(1)	
Ru(1)–C(2)	2.819(2)	2.11(1)	
Ru(1)–C(4)	2.13(1)	2.13(1)	
Ru(1)–C(102)	2.10(1)	2.19(2)	
Ru(1)–C(102)	2.21(1)	2.27(1)	
Ru(1)–C(104)	2.21(2)	2.16(1)	
Ru(2)–C(1)	2.04(1)	2.09(1)	
Ru(2)–C(9)	2.16(1)	2.14(1)	
Ru(2)–C(201)	2.22(1)	2.28(1)	
Ru(2)–C(203)	2.31(1)	2.26(1)	
Ru(2)–C(205)	2.25(1)	1.37(2)	
C(2)–C(3)	1.43(2)	1.40(2)	
	Angles (deg)		
Ru(2)–Ru(1)–C(1)	46.2(4)	Ru(2)–Ru(1)–C(2)	70.2(4)
Ru(2)–Ru(1)–C(3)	71.0(4)	Ru(2)–Ru(1)–C(4)	47.6(4)
C(1)–Ru(1)–C(2)	37.8(5)	C(1)–Ru(1)–C(3)	67.7(5)
C(1)–Ru(1)–C(4)	75.2(5)	C(2)–Ru(1)–C(3)	39.4(4)
C(2)–Ru(1)–C(4)	68.3(5)	C(3)–Ru(1)–C(4)	38.6(4)
Ru(1)–Ru(2)–C(1)	48.4(4)	Ru(1)–Ru(2)–C(4)	48.0(4)
Ru(1)–Ru(2)–C(9)	85.8(3)	Ru(1)–Ru(2)–C(10)	85.6(4)
C(1)–Ru(2)–C(4)	77.0(5)	C(1)–Ru(2)–C(9)	80.6(5)
C(1)–Ru(2)–C(10)	130.4(6)	C(4)–Ru(2)–C(9)	132.0(5)
C(4)–Ru(2)–C(10)	85.0(5)	C(9)–Ru(2)–C(10)	78.1(6)
Ru(1)–C(1)–Ru(2)	85.4(5)	Ru(2)–C(1)–C(2)	115(1)
C(1)–C(2)–C(3)	115(1)	C(2)–C(3)–C(4)	114(1)
Ru(1)–C(4)–Ru(2)	84.4(5)	Ru(2)–C(4)–C(3)	112.5(9)

^a Numbers in parentheses are estimated standard deviations.

Reaction of 7 with I₂ To Release the Coordinated Alkyne 11. While complex **2** easily releases the alkyne $(\text{Me}_3\text{SiC}\equiv\text{C})_2\text{C}=\text{CHSiMe}_3$ upon air oxidation,^{8a} analogous treatment of **7** gave a complicated reaction mixture and isolation of pure organic compounds was not successful. However, complex **7** readily reacted with I₂ at -78 °C to release the coordinated alkyne $\text{Me}_3\text{SiC}\equiv\text{CC}(\text{CO}_2\text{Me})=\text{CHSPri}$ (**11**), which was isolated as a colorless oil by silica gel chromatography and spectroscopically characterized (eq 2). The ¹H NMR spec-



trum of **11** exhibits the olefinic proton resonance at δ 7.63 together with the signals due to CO_2Me , SiMe_3 , and SPri groups, while the IR spectrum shows characteristic $\nu(\text{C}=\text{C})$ and $\nu(\text{C}=\text{O})$ bands at 2147 and 1711 cm^{-1} , respectively.²⁷

Experimental Section

General Considerations. The alkynes $\text{HC}\equiv\text{CCO}_2\text{R}$ ($\text{R} = \text{Me}$, Et, Bu^t), $\text{HC}\equiv\text{CTol}$, and $\text{HC}\equiv\text{CSiMe}_3$ commercially obtained were degassed and stored over molecular sieve 4A.

Table 10. Atomic Coordinates for 10b·ClCH₂CH₂Cl^{a,b}

	x	y	z	B_{eq} , \AA^2
Ru(1)	0.06348(8)	0.23350(5)	0.0289(1)	2.61(3)
Ru(2)	0.23515(8)	0.17622(5)	-0.07746(10)	2.40(2)
S(1)	0.0639(3)	0.1855(2)	-0.2075(3)	3.07(7)
P(1)	0.5834(4)	0.2031(3)	0.4976(4)	4.9(1)
F(1)	0.567(1)	0.2807(7)	0.560(2)	14.3(6)
F(2)	0.4613(10)	0.1822(10)	0.476(2)	13.7(6)
F(3)	0.576(1)	0.2223(7)	0.338(1)	11.9(5)
F(4)	0.587(1)	0.1809(9)	0.654(1)	12.7(5)
F(5)	0.7052(9)	0.2292(9)	0.518(1)	11.8(5)
F(6)	0.606(2)	0.1277(8)	0.440(2)	15.9(7)
O(1)	0.2038(8)	-0.0062(5)	0.090(1)	4.9(3)
O(2)	0.3242(7)	0.0576(5)	0.2596(9)	4.0(2)
C(1)	0.2206(9)	0.2526(6)	0.116(1)	2.5(3)
C(2)	0.275(1)	0.1913(7)	0.160(1)	3.2(3)
C(3)	0.2048(9)	0.1244(7)	0.128(1)	2.7(3)
C(4)	0.1016(10)	0.1318(6)	0.062(1)	2.7(3)
C(5)	-0.024(1)	0.0967(7)	-0.249(1)	3.6(3)
C(6)	-0.095(1)	0.1060(9)	-0.392(2)	5.5(4)
C(7)	0.036(1)	0.0278(7)	-0.262(2)	4.3(4)
C(8)	0.005(1)	0.3456(8)	0.106(3)	5.8(5)
C(9)	-0.004(2)	0.293(1)	0.210(2)	6.9(6)
C(10)	-0.078(2)	0.2364(9)	0.149(2)	6.2(6)
C(11)	-0.112(1)	0.2492(8)	0.012(2)	4.9(4)
C(12)	-0.060(1)	0.318(1)	-0.018(2)	5.8(5)
C(13)	0.062(2)	0.420(2)	0.141(4)	19(1)
C(14)	0.050(3)	0.305(2)	0.367(2)	17(1)
C(15)	-0.120(2)	0.171(1)	0.227(3)	15(1)
C(16)	-0.201(2)	0.212(2)	-0.099(4)	16(1)
C(17)	-0.085(2)	0.352(2)	-0.160(3)	12.6(10)
C(18)	0.329(1)	0.1024(7)	-0.214(1)	3.5(3)
C(19)	0.3999(10)	0.1424(7)	-0.098(1)	3.2(3)
C(20)	0.401(1)	0.2174(7)	-0.117(1)	3.5(3)
C(21)	0.325(1)	0.2251(7)	-0.242(1)	3.5(3)
C(22)	0.284(1)	0.1520(8)	-0.304(1)	4.0(4)
C(23)	0.316(1)	0.0210(8)	-0.248(2)	5.4(4)
C(24)	0.478(1)	0.1110(8)	0.011(1)	4.0(3)
C(25)	0.478(1)	0.2811(7)	-0.028(2)	4.2(3)
C(26)	0.304(1)	0.2950(9)	-0.313(2)	5.4(4)
C(27)	0.221(1)	0.1358(8)	-0.453(1)	4.5(4)
C(28)	0.2805(10)	0.3277(6)	0.151(1)	2.7(3)
C(29)	0.268(1)	0.3783(7)	0.050(1)	4.1(4)
C(30)	0.327(1)	0.4464(8)	0.078(2)	5.3(4)
C(31)	0.395(1)	0.4653(10)	0.205(2)	6.3(5)
C(32)	0.406(1)	0.4165(8)	0.309(2)	5.1(4)
C(33)	0.349(1)	0.3440(7)	0.282(1)	3.8(3)
C(34)	0.462(2)	0.5381(10)	0.237(2)	9.6(7)
C(35)	0.241(1)	0.0505(8)	0.154(1)	3.2(3)
C(36)	0.368(1)	-0.0093(8)	0.303(2)	4.9(4)
Cl(1)*	0.7251(9)	0.3962(7)	0.153(1)	19.0(5)
Cl(2)*	0.809(3)	0.524(1)	0.377(3)	23(1)
Cl(3)*	0.852(3)	0.459(2)	0.495(4)	27(1)
Cl(37)*	0.740(4)	0.438(4)	0.442(7)	24(2)
Cl(38)*	0.734(5)	0.383(2)	0.336(5)	20(1)

^a Numbers in parentheses are estimated standard deviations. ^b Asterisks denote the atoms in the solvate ClCH₂CH₂Cl. The atom Cl(3) is related to Cl(2) by the disorder in the crystal (50% occupancy each).

Solvents were dried by refluxing over Na/benzophenone ketyl (THF, benzene, toluene, hexane), P₂O₅ (dichloromethane), CaH₂ (acetonitrile), or Mg(OMe)₂ (methanol) and distilled just prior to use. All manipulations were performed using standard Schlenk-tube techniques. IR spectra were recorded on a Shimadzu 8100M spectrometer, while NMR spectra were obtained on a JEOL GX-400 or EX-270 spectrometer. Elemental analyses were performed on a Perkin-Elmer 2400II CHN analyzer or at the Elemental Analysis Laboratory, Department of Chemistry, The University of Tokyo.

(27) There were several Cp*Ru species in the reaction mixture. One minor product was identified as $\text{Cp}^*\text{Ru}(\mu_2\text{-I}_2)\text{RuCp}^*\text{I}$ by ¹H NMR data as well as X-ray diffraction analysis. Crystal data: orthorhombic, Cmca, $a = 13.641(4)$ Å, $b = 12.079(3)$ Å, $c = 15.628(3)$ Å, $Z = 4$, 1200 reflections, $R = 0.037$, $R_w = 0.047$.²⁸

(28) Kölle, U.; Kang, B.-S.; Englert, U. *J. Organomet. Chem.* 1989, 362, 383. This complex can be also obtained by treatment of [Cp*Ru($\mu_3\text{-Cl}$)₄] with LiOMe.^{6g}

Table 11. Selected Bond Distances and Angles for 10b-CICH₂CH₂Cl^a

Distances (Å)			
Ru(1)–Ru(2)	2.720(1)	Ru(1)–S(1)	2.291(3)
Ru(1)–C(1)	2.03(1)	Ru(1)–C(4)	2.01(1)
Ru(1)–C(8)	2.33(1)	Ru(1)–C(9)	2.21(1)
Ru(1)–C(10)	2.20(2)	Ru(1)–C(11)	2.23(2)
Ru(1)–C(12)	2.32(1)	Ru(2)–S(1)	2.367(3)
Ru(2)–C(1)	2.22(1)	Ru(2)–C(2)	2.19(1)
Ru(2)–C(3)	2.26(1)	Ru(2)–C(4)	2.36(1)
Ru(2)–C(18)	2.27(2)	Ru(2)–C(19)	2.23(1)
Ru(2)–C(20)	2.23(1)	Ru(2)–C(21)	2.21(1)
Ru(2)–C(22)	2.28(1)	S(1)–C(5)	1.88(1)
C(1)–C(2)	1.43(2)	C(2)–C(3)	1.44(2)
C(3)–C(4)	1.39(2)		
Angles (deg)			
Ru(2)–Ru(1)–S(1)	55.58(9)	Ru(2)–Ru(1)–C(1)	53.2(3)
Ru(2)–Ru(1)–C(4)	57.6(3)	C(1)–Ru(1)–C(4)	78.2(5)
Ru(1)–Ru(2)–S(1)	52.97(8)	Ru(1)–Ru(2)–C(1)	47.3(3)
Ru(1)–Ru(2)–C(2)	73.8(3)	Ru(1)–Ru(2)–C(3)	71.4(3)
Ru(1)–Ru(2)–C(4)	46.0(3)	S(1)–Ru(2)–C(1)	98.1(3)
S(1)–Ru(2)–C(2)	125.7(3)	S(1)–Ru(2)–C(3)	106.6(3)
S(1)–Ru(2)–C(4)	71.7(3)	C(1)–Ru(2)–C(2)	38.0(4)
C(1)–Ru(2)–C(3)	63.9(4)	C(1)–Ru(2)–C(4)	67.7(4)
C(2)–Ru(2)–C(3)	37.7(4)	C(2)–Ru(2)–C(4)	63.2(4)
C(3)–Ru(2)–C(4)	34.9(4)	Ru(1)–S(1)–Ru(2)	71.45(9)
Ru(1)–C(1)–Ru(2)	79.5(4)	Ru(1)–C(1)–C(2)	117.6(8)
C(1)–C(2)–C(3)	111(1)	C(2)–C(3)–C(4)	115(1)
Ru(1)–C(4)–Ru(2)	76.4(4)	Ru(1)–C(4)–C(3)	117.6(9)

^a Numbers in parentheses are estimated standard deviations.

Cp^{*}Ru(μ_2 -SPri)₂RuCp^{*} (**1**) was prepared *in situ* by treatment of Cp^{*}Ru(μ_2 -OMe)₂RuCp^{*}²⁸ with Me₃SiSPri (2 equiv) and used directly for the subsequent reactions with HC≡CCO₂R. Yields of complexes **5** were given on the basis of the amount of starting Cp^{*}Ru(μ_2 -OMe)₂RuCp^{*}.

Cp^{*}Ru(μ_2 -SPri)[η^2 : η^2 - μ_2 -C(CO₂Me)=CHSPri]RuCp^{*} (**5a**). To a toluene (5 mL) solution of **1** prepared *in situ* from Cp^{*}Ru(μ_2 -OMe)₂RuCp^{*} (392 mg, 0.733 mmol) and Me₃SiSPri (208 mg, 1.41 mmol) was added HC≡CCO₂Me (63 mg, 0.74 mmol) dropwise, and the mixture was stirred at room temperature for 6 h. After removal of the solvent *in vacuo*, the resulting dark brown solid was dissolved in hexane and loaded on an activated alumina column. The pink material initially obtained on washing with benzene/hexane (2/1) was discarded, and then a green band eluted with THF/hexane (1/19) was collected. Complex **5a** was obtained as a microcrystalline solid by evaporating the volatile materials from this eluate under reduced pressure (230 mg, 44%). IR (KBr): ν (C=O) 1684 cm⁻¹. ¹H NMR (C₆D₆, 400 MHz): δ 4.69 (s, 1H, C(CO₂Me)CHSPri), 3.72 (s, 3H, CO₂CH₃), 3.05, 2.52 (sep, 1H each, J = 6.7 Hz, SCHMe₂), 1.87, 1.75 (s, 15H each, C₅(CH₃)₅), 1.63, 1.50, 1.39, 1.01 (d, 3H each, J = 6.7 Hz, SCH(CH₃)₂). ¹³C{¹H} NMR (C₆D₆, 67.5 MHz): δ 176.90 (CO₂Me), 124.59 (C(CO₂Me)CHSPri), 91.41, 91.36 (C₅Me₅), 49.71 (CO₂CH₃), 44.00, 42.78, 40.08 (C(CO₂Me)CHSPri) and two SCHMe₂), 27.98, 26.57, 22.86, 20.86 (SCH(CH₃)₂), 10.82 (C₅(CH₃)₅). Anal. Calcd for C₃₀H₄₈O₂S₂Ru₂: C, 50.97; H, 6.84. Found: C, 51.32; H, 6.96.

Complexes **5b** and **5c** were obtained analogously.

Cp^{*}Ru(μ_2 -SPri)[η^2 : η^2 - μ_2 -C(CO₂Et)=CHSPri]RuCp^{*} (**5b**). Yield: 39%. IR (KBr): ν (C=O) 1682 cm⁻¹. ¹H NMR (C₆D₆, 400 MHz): δ 4.69 (s, 1H, C(CO₂Et)CHSPri), 4.50, 4.11 (dq, 1H each, J = 10.7, 7.0 Hz, CO₂CH₂CH₃), 3.06, 2.55 (sep, 1H each, J = 6.7 Hz, SCHMe₂), 1.90, 1.78 (s, 15H each, C₅(CH₃)₅), 1.64, 1.50, 1.41, 1.03 (d, 3H each, J = 6.7 Hz, SCH(CH₃)₂), 1.27 (t, 3H, J = 7.0 Hz, CO₂CH₂CH₃). ¹³C{¹H} NMR (C₆D₆, 67.5 MHz): δ 176.39 (CO₂Et), 124.54 (C(CO₂Et)CHSPri), 91.36, 91.30 (C₅Me₅), 58.64 (CO₂CH₂CH₃), 43.65, 42.92, 40.48 (C(CO₂Et)CHSPri) and two SCHMe₂), 27.93, 26.52, 22.95, 20.92 (SCH(CH₃)₂), 14.94 (CO₂CH₂CH₃), 10.88 (C₅(CH₃)₅). Anal. Calcd for C₃₁H₅₀O₂S₂Ru₂: C, 51.64; H, 6.99. Found: C, 51.36; H, 7.19.

Cp^{*}Ru(μ_2 -SPri)[η^2 : η^2 - μ_2 -C(CO₂Bu^t)=CHSPri]RuCp^{*} (**5c**).

Yield: 27%. Single crystals for the X-ray structural analysis were obtained by recrystallization from CH₂Cl₂–acetonitrile. IR (KBr): ν (C=O) 1678 cm⁻¹. ¹H NMR (C₆D₆, 400 MHz): δ 4.60 (s, 1H, C(CO₂Bu^t)CHSPri), 3.03, 2.61 (sep, 1H each, J = 6.7 Hz, SCHMe₂), 1.95, 1.79 (s, 15H each, C₅(CH₃)₅), 1.67 (s, 9H, CO₂C(CH₃)₃), 1.62, 1.50, 1.41, 1.03 (d, 3H each, J = 6.7 Hz, SCH(CH₃)₂). ¹³C{¹H} NMR (C₆D₆, 67.5 MHz): δ 175.30 (CO₂Bu^t), 126.32 (C(CO₂Bu^t)CHSPri), 91.33, 91.17 (C₅Me₅), 77.39 (CO₂C(CH₃)₃), 43.35, 42.76, 40.51 (C(CO₂Bu^t)CHSPri) and two SCHMe₂), 29.03 (CO₂C(CH₃)₃), 28.17, 26.60, 23.00, 21.35 (SCH(CH₃)₂), 11.12, 10.90 (C₅(CH₃)₅). Anal. Calcd for C₃₃H₅₄O₂S₂Ru₂: C, 52.92; H, 7.27; S, 8.56. Found: C, 52.47; H, 7.30; S, 8.05.

Cp^{*}Ru(μ_2 -SPri)[η^2 : η^3 - μ_2 -C(CO₂Me)CHC(CO₂Me)CHSPri]–RuCp^{*} (**6a**).

To a benzene (5 mL) solution of **5a** (94 mg, 0.13 mmol) was added HC≡CCO₂Me (28 mg, 0.34 mmol), and the reaction mixture was stirred at 50 °C for 44 h. After removal of the solvent *in vacuo*, the resulting dark brown solid was dissolved in hexane and loaded on a silica gel column. Elution with THF/hexane (1/19) afforded a yellow-green band, from which **6a** was obtained by evaporating the solvent *in vacuo* (77 mg, 75%). Single crystals for the X-ray structural analysis were available by recrystallization from hexane at –20 °C. IR (KBr): ν (C=O) 1715, 1686 cm⁻¹. ¹H NMR (C₆D₆, 400 MHz): δ 5.51 (d, 1H, J = 1.2 Hz, C(CO₂Me)CHC(CO₂Me)CHSPri), 4.54, 3.06 (sep, 1H each, J = 6.7 Hz, SCHMe₂), 3.73, 3.39 (s, 3H each, CO₂CH₃), 2.99 (d, 1H, J = 1.2 Hz, C(CO₂Me)CHC(CO₂Me)CHSPri), 1.82, 1.58, 1.42, 1.19 (d, 3H each, J = 6.7 Hz, SCH(CH₃)₂), 1.81, 1.53 (s, 15H each, C₅(CH₃)₅). Anal. Calcd for C₃₄H₅₂O₄S₂Ru₂: C, 51.62; H, 6.63. Found: C, 52.33; H, 6.99.

Complex **6a** can be prepared directly from **1** and HC≡CCO₂Me by the following procedure. To a THF (10 mL) solution of **1** prepared *in situ* from Cp^{*}Ru(μ_2 -OMe)₂RuCp^{*} (272 mg, 0.509 mmol) and Me₃SiSPri (215 mg, 1.45 mmol) was added HC≡CCO₂Me (182 mg, 2.17 mmol), and the mixture was stirred at room temperature for 24 h. The volatile materials were removed under reduced pressure, the resulting dark brown solid being dissolved in hexane and loaded on a silica gel column. Elution with THF/hexane (1/19) afforded a yellow-green band, from which **6a** was obtained by evaporating the solvent *in vacuo* (75 mg, 19%).

Cp^{*}Ru(μ_2 -SPri)[η^2 : η^3 - μ_2 -C(Tol)CHC(CO₂Me)CHSPri]–RuCp^{*} (**6b**).

To a toluene (5 mL) solution of **5a** (246 mg, 0.348 mmol) was added HC≡CTol (82 mg, 0.71 mmol), and the mixture was stirred at 50 °C for 15 h. After removal of the solvent *in vacuo*, the resulting dark brown solid was extracted with hexane. The extract was dried up, and the residue was crystallized from benzene–acetonitrile to give **6b** as greenish brown crystals (216 mg, 75%). IR (KBr): ν (C=O) 1684 cm⁻¹. ¹H NMR (C₆D₆, 400 MHz): δ 5.23 (d, 1H, J = 1.5 Hz, C(Tol)CHC(CO₂Me)CHSPri), 4.56, 3.13 (sep, 1H each, J = 6.7 Hz, SCHMe₂), 3.44 (s, 3H, CO₂CH₃), 2.93 (d, 1H, J = 1.5 Hz, C(Tol)CHC(CO₂Me)CHSPri), 2.26 (s, 3H, C₆H₄CH₃), 1.89, 1.66, 1.47, 1.27 (d, 3H each, J = 6.7 Hz, SCH(CH₃)₂), 1.62, 1.39 (s, 15H each, C₅(CH₃)₅). Anal. Calcd for C₃₉H₅₆O₂S₂Ru₂: C, 56.91; H, 6.86. Found: C, 56.85; H, 6.99.

Cp^{*}Ru(μ_2 -H)(μ_2 -SPri)[η^2 : η^2 - μ_2 -Me₃SiC≡CC(CO₂Me)=CHSPri]–RuCp^{*} (**7**). To a benzene (5 mL) solution of **5a** (175 mg, 0.248 mmol) was added HC≡CSiMe₃ (250 mg, 2.55 mmol), and the reaction mixture was stirred at room temperature for 6 days. After removal of the solvent *in vacuo*, the resulting brown solid was extracted with hexane. Crystallization of the evaporated residue from benzene–methanol gave **7** as dark red crystals (124 mg, 62%). IR (KBr): ν (C=O) 1686, ν (C=C) 1607 cm⁻¹. ¹H NMR (C₆D₅CD₃, 270 MHz, 22 °C): two sets of signals (A and B) are observed in about a 2:1 intensity ratio; set A, δ 7.66 (s, 1H, η^2 : η^2 - μ_2 -Me₃SiC≡CC(CO₂Me)=CHSPri), 3.56 (s, 3H, CO₂CH₃), 3.07, 1.88 (sep, 1H each,

$J = 7.1$ Hz, SCHMe_2 , 1.77 (s, 30H, $\text{C}_5(\text{CH}_3)_5$), 1.29, 1.10 (d, 6H each, $J = 7.1$ Hz, $\text{SCH}(\text{CH}_3)_2$), 0.46 (s, 9H, $\text{Si}(\text{CH}_3)_3$), -15.8 (s, 1H, $\mu_2\text{-H}$; set B, δ 7.69 (s, 1H, $\eta^2\text{-}\mu_2\text{-Me}_3\text{SiC}\equiv\text{CC}(\text{CO}_2\text{Me})=\text{CHSPri}^i$), 3.61 (s, 3H, CO_2CH_3), 2.98, 1.96 (sep, 1H each, $J = 7.1$ Hz, $\text{SCH}(\text{CH}_3)_2$), 1.79, 1.21 (d, 6H each, $J = 7.1$ Hz, $\text{SCH}(\text{CH}_3)_2$), 1.73 (s, 30H, $\text{C}_5(\text{CH}_3)_5$), 0.51 (s, 9H, $\text{Si}(\text{CH}_3)_3$), -15.9 (s, 1H, $\mu_2\text{-H}$). Anal. Calcd for $\text{C}_{35}\text{H}_{58}\text{O}_2\text{Si}_2\text{Ru}_2$: C, 52.21; H, 7.26. Found: C, 52.29; H, 7.62.

$\text{Cp}^*\text{I}_2\text{Ru}[\eta^2\text{-}\eta^4\text{-}\mu_2\text{-C}(\text{CO}_2\text{Me})\text{CHC}(\text{CO}_2\text{Me})\text{CH}] \text{RuCp}^*(8)$. To a benzene (5 mL) solution of **6a** (92 mg, 0.12 mmol) was added MeI (5 equiv), and the mixture was stirred at room temperature for 12 h. After removal of the solvent in vacuo, the resulting dark red solid was extracted with ether. The extract was dried up, and the residue was crystallized from CH_2Cl_2 -hexane at -78 °C to give **8** as reddish brown crystals (71 mg, 68%). IR (KBr): $\nu(\text{C=O})$ 1713, 1684 cm^{-1} . ^1H NMR (C_6D_6 , 400 MHz): δ 9.73 (d, 1H, $J = 1.8$ Hz, $\text{C}(\text{CO}_2\text{Me})\text{CHC}(\text{CO}_2\text{Me})\text{CH}$), 6.10 (d, 1H, $J = 1.8$ Hz, $\text{C}(\text{CO}_2\text{Me})\text{CHC}(\text{CO}_2\text{Me})\text{CH}$), 3.60, 3.51 (s, 3H each, CO_2CH_3), 1.86, 1.60 (s, 15H each, $\text{C}_5(\text{CH}_3)_5$). Anal. Calcd for $\text{C}_{28}\text{H}_{38}\text{O}_4\text{I}_2\text{Ru}_2$: C, 37.60; H, 4.28; I, 28.37. Found: C, 38.08; H, 4.49; I, 27.92.

$\text{Cp}^*\text{Me}_2\text{Ru}[\eta^2\text{-}\eta^4\text{-}\mu_2\text{-C}(\text{CO}_2\text{Me})\text{CHC}(\text{CO}_2\text{Me})\text{CH}] \text{RuCp}^*(9)$. To an ether (5 mL) solution of **8** (90 mg, 0.10 mmol) was added LiCuMe₂ (1 equiv) at -78 °C, and the mixture was slowly warmed to room temperature with stirring. After removal of the solvent in vacuo, the resulting black solid was extracted with benzene and loaded on a silica gel column. Elution with THF/hexane (1/19) afforded an orange band, from which **9** was obtained by evaporating the solvent under reduced pressure (33 mg, 49%). Single crystals for the X-ray structural analysis were obtained by recrystallization from toluene-acetonitrile. IR (KBr): $\nu(\text{C=O})$ 1713, 1700 cm^{-1} . ^1H NMR (C_6D_6 , 400 MHz): δ 8.55 (d, 1H, $J = 1.5$ Hz, $\text{C}(\text{CO}_2\text{Me})\text{CHC}(\text{CO}_2\text{Me})\text{CH}$), 6.52 (d, 1H, $J = 1.5$ Hz, $\text{C}(\text{CO}_2\text{Me})\text{CHC}(\text{CO}_2\text{Me})\text{CH}$), 3.65, 3.57 (s, 3H each, CO_2CH_3), 1.64, 1.27 (s, 15H each, $\text{C}_5(\text{CH}_3)_5$), 0.55, 0.54 (s, 3H each, Ru-CH₃). Anal. Calcd for $\text{C}_{30}\text{H}_{44}\text{O}_4\text{Ru}_2$: C, 53.72; H, 6.61. Found: C, 53.84; H, 6.68.

$[\text{Cp}^*\text{Ru}(\mu_2\text{-SPri}^i)\{\eta^2\text{-}\eta^4\text{-}\mu_2\text{-C}(\text{Tol})\text{CHC}(\text{CO}_2\text{Me})\text{CH}\}\text{RuCp}^*]\text{I}$ (10a). To a THF (5 mL) solution of **6b** (71 mg, 0.086 mmol) was added MeI (5 equiv) at -40 °C, and the mixture was slowly warmed to room temperature with stirring, during which time the initial greenish brown solution turned to a dark brown suspension. After removal of the solvent in vacuo, the resulting dark red solid was washed with benzene and crystallized from CH_2Cl_2 -ether to give **10a**^{1/2} CH_2Cl_2 as reddish brown crystals (42 mg, 53%). IR (KBr): $\nu(\text{C=O})$ 1717 cm^{-1} . ^1H NMR (CDCl_3 , 270 MHz, 22 °C): δ 7.13, 6.99 (d, 2H each, $J = 7.8$ Hz, aryl), 6.17, 6.04 (d, 1H each, $J = 2.7$ Hz, $\text{C}(\text{Tol})\text{CHC}(\text{CO}_2\text{Me})\text{CH}$ and $\text{C}(\text{Tol})\text{CHC}(\text{CO}_2\text{Me})\text{CH}$), 3.81 (s, 3H, CO_2CH_3), 2.99 (sep, 1H, $J = 6.9$ Hz, SCHMe_2), 2.36 (s, 3H, $\text{C}_6\text{H}_4\text{CH}_3$), 1.75 (pseudo d, 6H, $J = 7.6$ Hz, $\text{SCH}(\text{CH}_3)_2$), 1.53 (s, 30H, $\text{C}_5(\text{CH}_3)_5$). Anal. Calcd for $\text{C}_{36}\text{H}_{49}\text{O}_2\text{SiRu}_2^{1/2}\text{CH}_2\text{Cl}_2$: C, 47.79; H, 5.49; S, 3.49. Found: C, 47.84; H, 5.50; S, 3.75.

The corresponding PF_6^- salt **10b** was prepared as follows. Reddish brown crystals of **10a**^{1/2} CH_2Cl_2 (151 mg, 0.165 mmol) were dissolved in CH_2Cl_2 (3 mL), and aqueous NaPF_6 (1.16 g, 7 mL) was added. The resulting mixture was stirred for 2 h, and then the aqueous layer was removed by a syringe. After dilution by additional CH_2Cl_2 (5 mL), the solution was dried over MgSO_4 . The mixture was filtered and the residue was extracted with CH_2Cl_2 (2 mL × 3). The extracts were combined with the filtrate and evaporated to dryness. Recrystallization of the remaining solid from CH_2Cl_2 -ether resulted in the isolation of **10b**- $\text{ClCH}_2\text{CH}_2\text{Cl}$ (74 mg, 45%). IR (KBr): $\nu(\text{C=O})$ 1715 cm^{-1} . ^1H NMR (CDCl_3 , 270 MHz, 22 °C): δ 7.11, 6.97 (d, 2H each, $J = 7.8$ Hz, aryl), 6.17, 5.99 (d, 1H each, $J = 2.7$ Hz, $\text{C}(\text{Tol})\text{CHC}(\text{CO}_2\text{Me})\text{CH}$ and $\text{C}(\text{Tol})\text{CHC}(\text{CO}_2\text{Me})\text{CH}$), 3.80 (s, 3H, CO_2CH_3), 2.97 (sep, 1H, $J = 6.9$ Hz, SCHMe_2), 2.34 (s, 3H, $\text{C}_6\text{H}_4\text{CH}_3$), 1.73 (pseudo d, 6H, $J = 7.6$ Hz, $\text{SCH}(\text{CH}_3)_2$), 1.49 (s, 30H, $\text{C}_5(\text{CH}_3)_5$).

$\text{Me}_3\text{SiC}\equiv\text{CC}(\text{CO}_2\text{Me})=\text{CHSPri}^i$ (**11**). To an ether (7 mL) solution of **7** (105 mg, 0.130 mmol) was added I_2 (33 mg, 0.13 mmol) at -78 °C, and the mixture was slowly warmed to 0 °C with stirring for 11 h. The resulting dark brown suspension was filtered, and the residue was extracted with ether (10 mL × 2). The extracts were combined with the filtrate, and the solvent was removed under reduced pressure. Then the resulting brown residue was extracted with hexane and loaded on a silica gel column. Elution with $\text{EtOAc}/\text{hexane}$ (1/4) afforded a light yellow band, from which **11** was obtained by evaporating the solvent in vacuo (18 mg, 54%). IR (Nujol): $\nu(\text{C}\equiv\text{C})$ 2147, $\nu(\text{C=O})$ 1711 cm^{-1} . ^1H NMR (C_6D_6 , 270 MHz): δ 7.63 (s, 1H, $\text{Me}_3\text{SiC}\equiv\text{CC}(\text{CO}_2\text{Me})=\text{CHSPri}^i$), 3.41 (s, 3H, CO_2CH_3), 2.35 (sep, 1H, $J = 6.8$ Hz, SCHMe_2), 0.84 (d, 6H, $J = 6.8$ Hz, $\text{SCH}(\text{CH}_3)_2$), 0.30 (s, 9H, $\text{Si}(\text{CH}_3)_3$). MS (high resolution): calcd for $\text{C}_{12}\text{H}_{20}\text{O}_2\text{SiS}$ m/z 256.1006 (M^+), found m/z 256.0980 (M^+).

X-ray Crystallographic Studies. Crystals suitable for the X-ray analysis were sealed in glass capillaries under Ar and mounted on a four-circle diffractometer equipped with a graphite monochromator. Intensity data were corrected for Lorentz-polarization effects and for absorption. Details of the X-ray crystallography for **5c**, **6a**, **7**, **9**, and **10b**- $\text{ClCH}_2\text{CH}_2\text{Cl}$ are summarized in Table 1. In the structure factor calculations, hydrogen atoms were not included unless otherwise noted. The molecular structures were drawn by using the program ORTEP.²⁹

5c, **7**, and **10b**- $\text{ClCH}_2\text{CH}_2\text{Cl}$. Cell constants and orientation matrices for data collection were obtained from a least-squares fit of 25 machine-centered reflections in the range $48 < 2\theta < 54^\circ$ (for **5c**), $27 < 2\theta < 31^\circ$ (for **7**), or $39 < 2\theta < 41^\circ$ (for **10b**- $\text{ClCH}_2\text{CH}_2\text{Cl}$). The intensities of 3 representative reflections were measured every 150 reflections. For **5c** and **10b**- $\text{ClCH}_2\text{CH}_2\text{Cl}$, no significant decay was observed for the standard reflections. In the case of **7**, the intensities of the standard reflections decreased by 28% over the course of data collection and a linear correction factor was applied to the reflection data as a function of data collection number. All calculations were performed by using the TEXSAN crystallographic software package.³⁰ The structures were solved by a combination of Patterson methods and Fourier techniques and refined by full-matrix least-squares techniques. All non-hydrogen atoms were refined anisotropically for **5c**, while only the Ru, S, Si, and O atoms were refined by using anisotropic temperature factors for **7**. For **10b**- $\text{ClCH}_2\text{CH}_2\text{Cl}$, anisotropic refinements were undertaken for all non-hydrogen atoms. In the final Fourier map, one Cl atom attached to C(37) was located at two disordered positions with almost similar electron densities and was refined as Cl(2) and Cl(3) with 50% occupancy each.

6a. The orientation matrices and unit cell parameters were derived from a least-squares fit of 25 machine-centered reflections with 2θ values between 20 and 25°. No significant decay was observed for 3 check reflections measured every 100 reflections. Structure solution and refinement were performed by using the UNIX-III program package at the computer center of The University of Tokyo. The Ru atoms were found by direct methods (SHELXS 86).³¹ The remaining non-hydrogen atoms were located by subsequent block-diagonal least-squares refinement and difference Fourier maps. All non-hydrogen atoms were refined anisotropically.

9. The orientation matrices and unit cell parameters were derived from a least-squares fit of 25 machine-centered reflections with 2θ values between 20 and 30°. Three check reflections measured every 150 reflections showed no signifi-

(29) Johnson, C. K. ORTEP-II, A FORTRAN Thermal Ellipsoid Plot Program; Oak Ridge National Laboratory: Oak Ridge, TN, 1976.

(30) TEXSAN: Crystal Structure Analysis Package; Molecular Structure Corp., 1985 and 1992.

(31) Sheldrick, G. M. SHELXS86, Program for Crystal Structure Determination; University of Göttingen, Göttingen, Germany, 1986.

cant decay during data collection. All calculations were performed by using the TEXSAN crystallographic software package.³² The structure was solved by the direct methods program MITHRIL.³³ All non-hydrogen atoms were refined anisotropically by full-matrix least-squares techniques. Hydrogen atoms were placed at calculated positions and were included in the final stage of refinements with fixed parameters.

(32) TEXSAN: TEXRAY Structure Analysis Package; Molecular Structure Corp., 1985.

(33) Gilmore, C. J. MITHRIL: An Integrated Direct Methods Computer Program; University of Glasgow, Glasgow, Scotland, 1984.

Acknowledgment. We thank the Ministry of Education, Science and Culture of Japan for financial support.

Supplementary Material Available: A figure showing the molecular structure of **10b**·ClCH₂CH₂Cl, tables of thermal parameters and complete lists of bond distances and angles for **5c**, **6a**, **7**, **9**, and **10b**·ClCH₂CH₂Cl, and a table of hydrogen atom coordinates for **9** (26 pages). Ordering information is given on any current masthead page.

OM9400917